

THEMODYNAMICS LIMITS AND ENERGETIC ANALYSIS
OF CHEMICAL PROCESS INTENSIFICATION

A Thesis

by

CHANGYEONG SONG

Submitted to the Office of Graduate and Professional Studies of
Texas A&M University
in partial fulfillment of the requirements for the degree of

MASTER OF SCIENCE

Chair of Committee,
Committee Members,

M.M. Faruque Hasan
Stratos Pistikopoulos
Ying Li

Interdepartmental Program Chair,

Stratos Pistikopoulos

August 2018

Major Subject: Energy

Copyright 2018 Changyeong Song

ABSTRACT

Many energy technologies are based on the chemical process such as conversion, separation and storage within a single flow-sheet. This chemical process can be intensified by combining several operation units in a single unit, which leads to a fundamentally cleaner, safer, more compact and more energy-efficient technology.

However, for many chemical technologies, the theoretical limit of intensification is currently unknown. In this project, fundamental concepts of thermodynamics (e.g., 1st law, 2nd law, enthalpy and entropy calculation, Gibbs free energy minimization, mole balance and stoichiometric coefficient, heat, work, and exergy) are precisely applied, also improving the constraints of NLP formulation model. To this end, ultimate goal of this work is to achieve the maximum possible with accurately describing actual chemical phenomenon.

This work can be also applied for many different chemical models such as fuel processing plants and energy sectors. First analysis is conducted on the methane reforming alternatives in syngas production model with small number of chemical species and reaction pathways, and next, the model is expanded to include various conversion routes of chemicals; methanol synthesis and ethane reforming are analyzed.

CONTRIBUTORS AND FUNDING SOURCES

This work was supervised by a thesis committee consisting of Professor Faruque Hasan and Stratos Pistikopoulos of the Energy institute and Professor Ying Li of the Department of Mechanical Engineering.

There are no outside funding contributions to acknowledge related to the research and compilation of this document.

NOMENCLATURE

NLP	Non Linear Programming
CCS	Carbon Capture and Storage
DR	Dry Reforming
POX	Partial Oxidation
SMR	Steam Methane Reforming
CDSR	Combined Dry and Steam Reforming
PODR	Partial Oxidation and Dry Reforming
CR	Combined Reforming with CO ₂ , Methane, Oxygen, and Steam
Tri reforming	Same as CR
WGS	Water Gas Shift
RWGS	Reverse Water Gas Shift
SR	Syngas Ratio
FT	Fischer-Tropsch Process
DME	Dimetheylether
P	Pressure
T	Temperature
GHG	Green House Gas

TABLE OF CONTENTS

	Page
ABSTRACT	ii
CONTRIBUTORS AND FUNDING SOURCES.....	iii
NOMENCLATURE.....	iii
TABLE OF CONTENTS	v
LIST OF FIGURES.....	vii
LIST OF TABLES	viii
CHAPTER I INTRODUCTION	1
1.1 CO ₂ Utilization and Syngas/Synthesis-gas Production.....	1
1.2 Research Objectives and Thesis Outline.....	7
CHAPTER II LITERATURE REVIEW.....	7
2.1 Combined Reformers for Methane; PODR, CDSR, and CR.....	8
2.2 Methanol Synthesis from Syngas.....	11
CHAPTER III ENERGETIC ANALYSIS OF CO ₂ UTILIZATION AND CH ₄ REFORMING	13
3.1 Enthalpy and Entropy Calculation	14
3.2 Gibbs Free Energy; Calculation, Regression and Minimization.....	16
3.3 Mole balances and Reaction pathways	20
3.4 Objective Variables.....	24
3.5 Coke-deposition; Reaction Kinetics and Gibbs Free Minimization	27
3.6 Nonlinear (NLP) Optimization Model.....	28

3.7 Results for CO ₂ Utilization and Methane Reforming at Equilibrium Conditions	33
CHAPTER IV EXTENSIVE STUDIES FOR METHANOL AND ETHANE	37
4.1 Novel Constraints for Gas Sepataion and Methanol Synthesis	37
4.2 Novel Constraints for Linear Dependence of Reacton Pathways	38
4.3 Results for Methanol Synthesis and Ethane Reforming	42
CHAPTER V CONCLUSION	46
REFERENCES	47
APPENDIX A	50
APPENDIX B	51
APPENDIX C	54

LIST OF FIGURES

FIGURE		Page
1	Possible CO ₂ Utilization trend in various products and precedures.....	2
2	Pathways bewond syngas depicting various conversion routes	4
3	Results from the energetic analysis for syngas production	33
4	Realistic reaction pathways in ethane tri-reforming	38
5	Results from the energetic analysis for methanol synthesis and reforming	42

LIST OF TABLES

TABLE	Page
2.1 Reaction enthalpy of methane reforming in regard to product temperature	7
2.2 Energy generation Per CO ₂ emission for primary energy resources.....	7
2.3 Reaction enthalpy of methanol synthesis in regard to product temperature	12
B.1 Stoichiometric coefficients in methane reforming	51
B.2 Stoichiometric coefficients in ethane reforming	51
C.1 Enthalpy of the reaction pathways in regard with product temperature	54
C.2 Linear Regression for standard Gibbs free energy of formation.....	54

CHAPTER I

INTRODUCTION

1.1 CO₂ Utilization and Syngas/Synthesis-gas Production

CO₂ Utilization More than other chemical models, thermodynamic limits of CO₂ utilization and syngas production should be explored first. This chemical process intensification can give the light on the global challenges related with CO₂ emission. Chemical model of CO₂ and syngas is the starting point of the thesis development.

CO₂ capture and storage (CCS) of power plant flue gases has gained worldwide interest in terms of global climate change. However, U.S. Department of Energy (DOE) estimated that “CCS technologies would add around 80 percent to the cost of electricity for a new pulverized coal plant, and around 35 percent to the cost of electricity for a new advanced gasification-based plant.” (1)

Economic and population growth continue to be the most important factors behind increases in CO₂ emissions from fossil fuel combustion. The escalation of anthropogenic CO₂ emissions linked to global warming has attracted global efforts to find new and better ways of meeting the world’s growing energy demand, while simultaneously reducing greenhouse-gas (GHG) emissions (2). Despite a growing number of climate change mitigation initiatives and policies, global GHG emissions grew on average by 2.2% carbon dioxide equivalent (CO₂ eq) per year from 2000 to 2010 compared to 1.3% CO₂ eq per year from 1970 to 2000 (3). Carbon dioxide emissions from fossil fuel combustion and industrial processes contributed about 78% of the total GHG emission increase from 1970 to 2010. In 2010 fossil fuel-related CO₂ emissions reached 32 (\pm 2.7) Gt/y, and grew

further by about 3% between 2010 and 2011 and by about 1–2% between 2011 and 2012 (3).

Syngas/Synthesis-gas Production As shown in the figure 1 and 2, reaction pathways beyond syngas and synthesis gas can be the powerful tool to offset the high cost of CCS. Syngas is located in the mid of carbon dioxide utilization and value-added products. For example, Fischer-Tropsch (FT) is well-known syngas upgrading process to produce e.g. gasoline, diesel, jet fuels, olefin, waxes, and so forth.

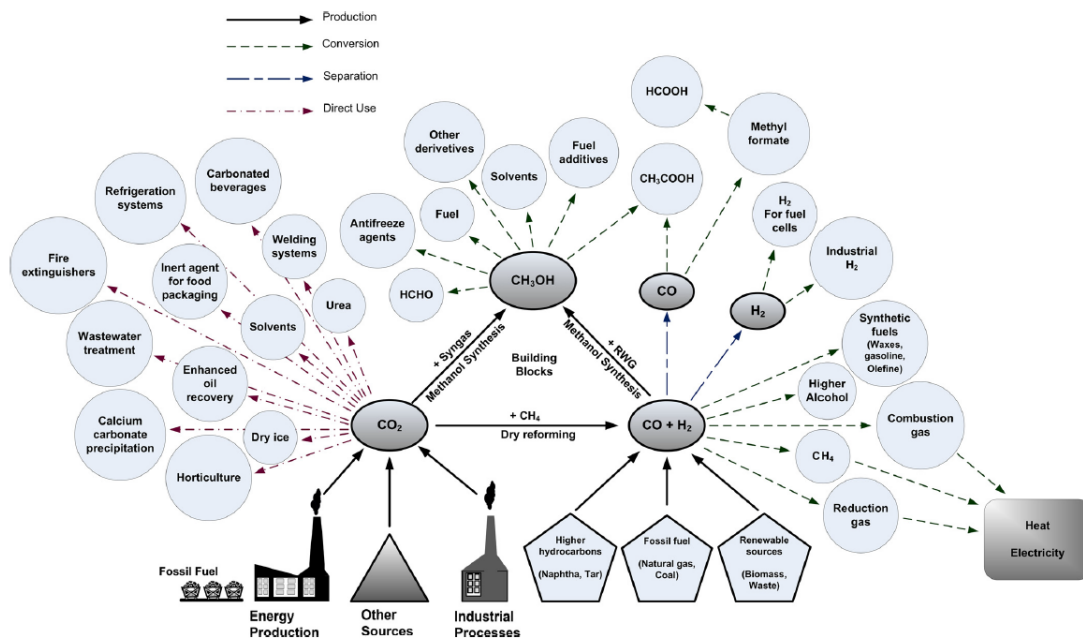


Figure 1. Possible CO₂ utilization trend in various products and procedures. (Milani et al, 2015) (4)

Utilizing the greenhouse gas CO₂ as a feedstock in chemical processing could offer alternative solutions to long-term storage. Large-scale production of light hydrocarbons such as methanol (MeOH) is one of the predominant and sensible schemes for such utilization. This proposal will not only recycle the CO₂ gas within methanol synthesis process, but will also reduce the uptake of raw materials such as natural gas (NG) and reduce the greenhouse-gas (GHG) emissions of a comparable stand-alone NG-based methanol synthesis plant.

Methanol (methyl alcohol, CH₃OH or MeOH) is the simplest liquid hydrocarbon that can be regarded as a fuel, a hydrogen carrier or a feedstock for producing more complex chemical compounds. Methanol production can be achieved by using fossil fuel sources (NG, coal) or renewable sources (biomass, waste wood, atmospheric CO₂). More than 80% of the MeOH produced worldwide is obtained from NG (5). However, the process of producing MeOH from NG only is often associated with extremely high GHG emission.

Methanol synthesis is a mature process developed from a steady-state kinetic model for hydrogenation of CO₂ and reverse water-gas shift (RWGS) reactions on a commercial Cu/ZnO/Al₂O₃ catalyst. In order to express optimal feed composition of ideal gas for methanol production from synthesis gas, stoichiometric number (SN) is defined as below. Optimal feed composition is at which SN is equal to 2. (5)

$$SN = \frac{n_{H_2} - n_{CO_2}}{n_{CO} - n_{CO_2}}$$

Methanol is one of the most important raw chemical materials. About 85% of the methanol produced is used in the chemical industry as a building block or solvent for synthesis and the remainder is used in the fuel and energy sector (6). Methanol is mainly

used in the production of formaldehyde (35%), methyl tertiary-butyl ether (MTBE) (25%) and acetic acid (9%), respectively (7). Methanol can also be blended with different grades of gasoline for existing automobiles and hybrid flexible vehicles. One big advantage is that methanol can be produced in the same quality from fossil raw materials and from renewable primary energy carriers.

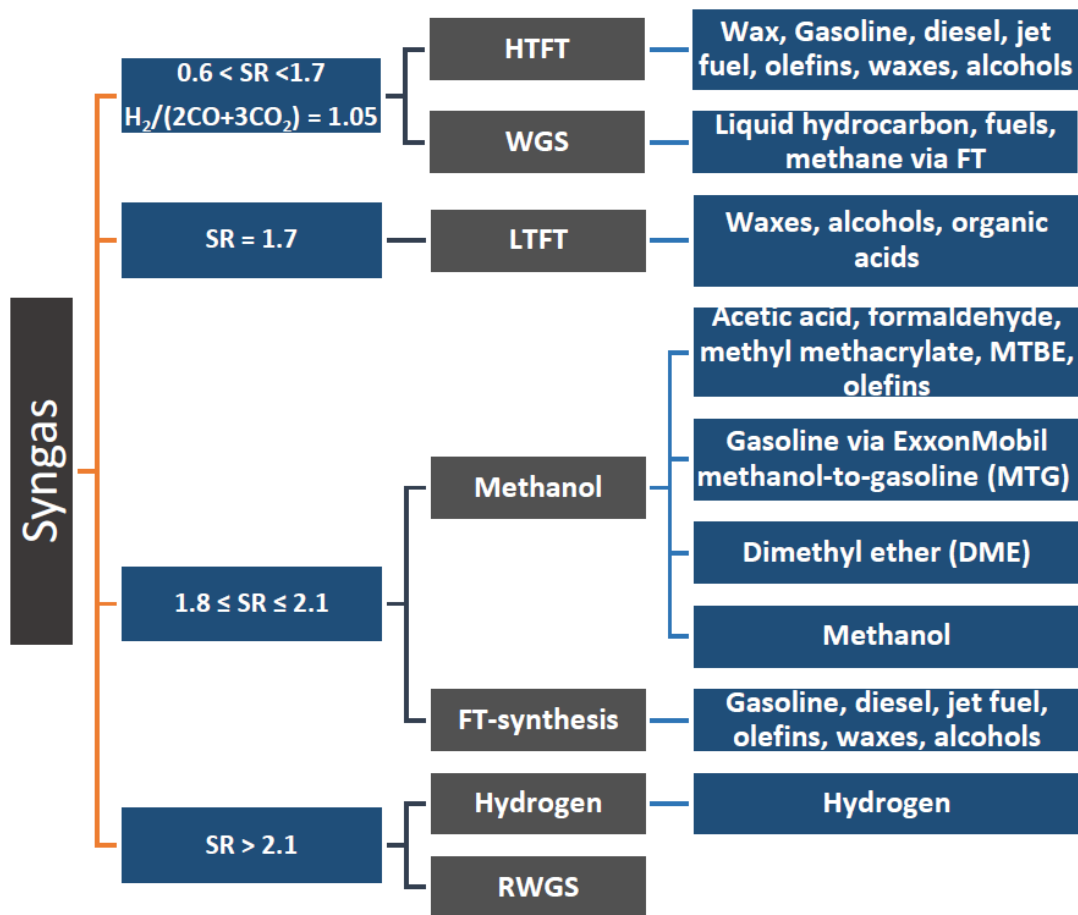
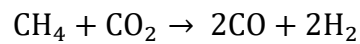


Figure 2. Pathways beyond syngas depicting various conversion routes.

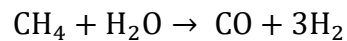
(Balasubramanian P, 2017) (8)

Different reforming options, so called alternatives, are available to produce syngas, utilize CO₂, or both; and each of which can be distinguished based on chemical species used in feed flow. Following reaction formulations can be occurred by the feed molecules in the alternatives. Reforming alternatives are more explained in the chapter 2.

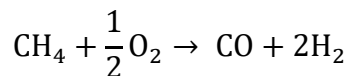
- **DR (Dry Reforming)**



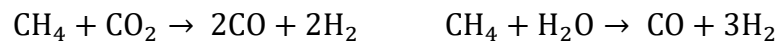
- **SMR (Steam Methane Reforming)**



- **POX (Partial Oxidation)**



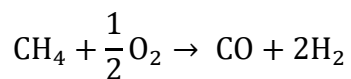
- **CDSR (Combined Dry and Steam Reforming)**



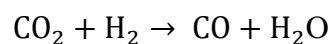
- **PODR (Combined Dry and Partial Oxidation)**



- **CR (Combined Reforming of Methane, Carbon Dioxide, Water, and Oxygen)**



- **RWGS (Reverse Water Gas Shift)**



In order to express optimal feed composition for methanol production from syngas, syngas ratio is defined as below. Because of stoichiometric coefficients, syngas ratio of 2 is desirable.

$$SR \text{ (or } R^{SG}) = \frac{n_{H_2}}{n_{CO}} \quad (1.1.1)$$

1.2 Research Objectives and Thesis Outline

- Literature review of the alternatives and CCS.
- Development of NLP (non-linear-programming) formulation with novel constraints and precise approaches in thermodynamics; the development covers Gibbs free minimization, mole balances with extent of reaction, and linear dependence of reaction pathways.
- Optimization Strategy; finding global optimal solutions through developing the strategy properly.
- Case study on CO₂;

Obtain ¹⁾ Realistic values of conversion and syngas yield

²⁾ Optimal route and conditions for the maximum utilization of CO₂.

- Extensive Case Studies on Different Systems

1) Conversion Routes of Methanol

2) Ethane Reforming

CHAPTER II

LITERATURE REVIEW

Primary reformers are group of reactions DR, POX, and SMR as explained in chapter 1. All these combined reformers take an advantage of producing various range of syngas ratio, which is defined by hydrogen moles over carbon monoxide moles. Reaction enthalpy with respect to final temperature is calculated as below table 2.1 in order to analyze reformers thermodynamically.

	Enthalpy of Reaction (kJ/mol) with respect to T ₂					comment
	298.15 K	600 K	900 K	1200 K	1500 K	
DR	247.359	279.864	315.657	353.442	392.920	Endothermic
POX	-35.625	-10.600	16.265	44.438	73.781	Swing
SMR	206.203	240.000	275.835	313.288	352.234	Endothermic
RWGS	41.156	59.152	79.504	101.596	125.286	Endothermic

Table 2.1 Reaction enthalpy of methane reforming in regard to product temperature

	CO ₂ emission (moles) / Million Btu	kJ / CO ₂ emission (moles)
Coal (anthracite)	228.6	448.3
Diesel fuel and heating oil	161.3	635.3
Gasoline (without ethanol)	157.2	651.9
Propane	139	737.2
Natural gas	117	875.9

Table 2.2 Energy generation per CO₂ emission for primary energy resources (9)

In the table 2.2, energy generation per CO₂ emission for primary energy resources is theoretically identical to combustion energy of the resources. It is important to consider this energy generation as a guideline for indirect emissions of carbon dioxide from the combined methane reforming reactors.

2.1 Combined Reformers for Methane; PODR, CDSR, and CR

In this subchapter, combined reformers of methane are explained in terms of brief history, novel concept proposal, thermodynamic simulation, catalytic-reforming experiment, and optimization. Advantages and reaction conditions are analyzed and compared together.

Combined Partial Oxidation and Dry Reforming of Methane (PODR); It has been observed that the coupling of the endothermic dry reforming with the exothermic partial oxidation can significantly reduce hot spots in the catalyst bed as well as reduce the loss of catalyst activity with time. (10)

The dry reforming reaction is highly endothermic and requires temperatures above 700 K for substantial reaction to occur. It is important to consider the sensible energy, which is spent in heating reactors, because it would lead to indirect emissions of carbon dioxide; specifically saying, the primary aim of our research would be contradicted if the sensible energy per moles of CO₂ utilized is larger than moles of CO₂ emission derived by primary resource consumption as shown in Table 2.2.

Under the conditionst that reactor temperature is 700 K, POX of methane is an exothermic reaction and can be combined with DR of methane to raise the reaction temperature to facilitate the dry reforming. Theoretically, DR produces mixtures of which

syngas ratio is one, and POX produces mixtures of which syngas ratio is two. Combined reformer PODR with only DR and POX is able to produce mixtures having the range of syngas ratio from 1 to 2.

It is important to consider that not only DR and POX, but also Combustion, WGS, and RWGS can happen at PODR. Technically saying, SMR or other reactions can be also occurred by water, a byproduct of the former reactions. In addition, due to RWGS which consumes hydrogen and produces carbon monoxide, syngas ratio lower than 1. Because WGS and combustion have very low reaction constant at high temperature, PODR is mainly composed of DR, POD, and RWGS.

Amin and Yaw (11) performed thermodynamic analysis of PODR, and this was done by total Gibbs energy minimization using Lagrange's undetermined multiplier method. The results showed that the addition of oxygen to dry reforming improved the methane conversion, H₂ and H₂O yields, and syngas ratio, but decreased the CO₂ conversion and CO yield.

In PODR, two oxidants, namely CO₂ and O₂, compete to oxidize methane. However, partial oxidation dominates over dry reforming. An increment in CO₂/CH₄ feed ratio results in the loss of CO₂ conversion while producing more H₂O. (11) Since the CO₂ conversion is of primary interest, PODR operations need to be optimized to increase the CO₂ utilization. Equilibrium CO₂ conversion increases with temperature but decreases with CO₂/CH₄ ratio. Higher temperatures are favorable to achieve H₂/CO ratio of syngas close to one and high conversion.

Combined Dry Reforming and Steam Reforming of Methane (CDSR); As discussed before, dry reforming of methane produces syngas of ratio 1, while utilizing CO₂. Steam reforming produces syngas in the ratio close to 3. Thus, combining these two reactors, the syngas ratio can be adjusted to be around 2, while utilizing CO₂, whereas other reactors such as POX that produce similar SR but decrease the CO₂ conversion.

As explained in chapter 1, the syngas ratio around 2 is suitable for methanol synthesis, and methanol is a chemical of commercial importance and can offset the cost of CO₂ utilization. Therefore, CDSR with reasonable operating conditions, could produce an desirable products and could lead to a potential reduction in reactor size and catalyst cost.

Tri-Reforming (Combined Reforming) of Methane (CR); Tri-reforming is the combination of DR, SMR and POX. This reactor has the combined advantages of multiple bi-reforming reactors such as achieving desirable syngas ratios and reduction of coke deposition (12). Though tri-reforming consists of the three independent reactions

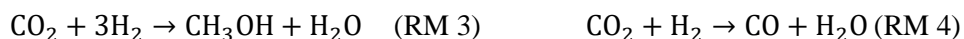
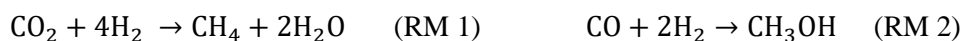
Song et al. (2004) (13) proposed this novel concept of tri-reforming and the advantages mentioned were demonstrated in a laboratory-scale fixed-bed flow reactor 91. Cho et al. (2009) (14) developed a first principle model for the tri-reforming of natural gas to produce DME. The model consisted of two regions, one homogeneous and one heterogeneous. The two sections were one-dimensional steady state plug-flow reactor models. The models were built on Jacobian dynamic modeling and optimization software and is compared with an equilibrium model. The reactor optimal length for maximum hydrogen and maximum carbon monoxide production are found by fixing the other operational variables. (14)

Depending on the reaction conditions of feed composition and temperature, it is important to notice that characteristics of PODR can be also occurred at CR or CDSR, vice versa. For example, in CR, relatively high temperature and high oxygen/water feed ratio is required when syngas ratio is close one so as to become thermodynamically favorable state, as same as what explained in PODR. In other words, it can be said that this reactor is mainly composed of large portion of PODR and small portion of CDSR. High oxygen/water feed ratio in CDSR is explained again in chapter 3.

Reverse Water Gas Shift (RWGS); As the name suggests, RWGS is the reverse of the water gas shift reaction that we have discussed previously. This reaction does not require very high operational temperatures and is favored by Ni catalysts. This reaction utilizes CO_2 .

Compared to the other reforming reactors, there is considerably lesser research done on reverse water gas shift. This is possibly because water gas shift or reverse water gas shift reactions follow other reforming reactions or are used to upgrade the quality of the hydrocarbon product rather than being used as an individual reactor. Joo et al. (1999) (15) compared the direct hydrogenation of carbon dioxide to methanol and the case where reverse water gas of shift precedes the methanol synthesis on a Cu-based catalyst and found that the production of methanol was higher by 29% for the latter case and the recycle volume for the methanol synthesis reactor was considerably lower when the feed composed of CO, unreacted CO_2 and H_2 (15).

2.2 Methanol Synthesis from Syngas



Above four reactions are main steps for methanol synthesis.

	Enthalpy of Reaction (kJ/mol) with respect to T2					Comment
	298.15 K	600 K	900 K	1200 K	1500 K	
RM 1	-206.10	-182.22	-152.64	-118.12	-79.62	Exothermic
RM 2	-90.14	-72.63	-49.17	-21.21	9.69	Swing
RM 3	-48.98	-20.96	13.93	54.36	98.82	Swing
RM 4	41.156	59.152	79.504	101.596	125.286	Endothermic

Table 2.3 Reaction enthalpy of methanol synthesis in regard to product temperature

The first catalyst used for large scale production of methanol was developed by BASF in 1923. This was a $\text{Cr}_2\text{O}_3/\text{ZnO}$ catalyst and the reaction was carried out at about 30 MPa and 573–673 K. Later in 1960, the availability of technology to produce sulphur free synthesis gas made it possible to use the more selective $\text{Cu}/\text{ZnO}/\text{Al}_2\text{O}_3$ catalyst. This catalyst made it possible for synthesis gas hydrogenation to methanol to be carried out under milder conditions at lower pressures of 6–8 MPa and temperatures in the range of 523–553 K. This is called the ICI low pressure process. Currently, $\text{Cu}/\text{ZnO}/\text{Al}_2\text{O}_3$ based catalysts are used for syngas hydrogenation to methanol. This has a very high selectivity (99.9%) toward methanol. However these cannot be used at temperatures above 573 K and are highly sensitive towards poisoning by sulphur.

The two reactions (RM 2) and (RM 3) are hydrogenation of CO and CO₂ to methanol, i.e. methanol synthesis reactions while the third is the reverse water gas shift reaction (RWGS). The reactions are reversible and are limited by thermodynamics. The methanol synthesis reactions are exothermic and proceed with decrease in number of moles. Hence lower temperatures and higher pressures drive the equilibrium of the methanol synthesis reactions forward in accordance with Le Chatelier's principle. The reverse water gas shift reaction is an endothermic reaction and proceeds with no change in the number of moles.

CHAPTER III

ENERGETIC ANALYSIS OF CO₂ UTILIZATION AND CH₄ REFORMING

This section consists of 5 subchapters, each of which explains the following contents

- How to calculate the Enthalpy and Entropy?
- How to estimate the number of moles in the feed and equilibrium products?
- How to calculate Minimum Required Energy?
- How to set the NLP Optimization Model?
- How to analyze the results from the NLP Optimization Model?

Based on these contents, the final goal of this chapter is figure out the following questions for a given syngas (H₂ to CO) ratio.

- What is the theoretically minimum required energy; the energy needed to convert CO₂ into syngas using different reforming alternatives
- What is the maximum CO₂ utilization; the ratio of the final CO₂ composition to the feed CO₂ composition
- What is the maximum achievable syngas selectivity; the ratio of the (H₂ + CO) combined composition to the summation of product composition

These questions, which become the objective variables in the NLP Optimization model, are addressed based on the following thermodynamic analysis; 'Enthalpy and Entropy Calculation' and 'Gibbs Free Minimization'.

3.1 Enthalpy and Entropy Calculation

The chemical model in this thermodynamics analysis is supposed to be a fully reversible system at which the amount of change in enthalpy, from its initial state of T_1 and P_1 to the final state of T_2 and P_2 , is the energy consumption to convert chemical species set to another set; in addition, this energy change is defined as the theoretically ‘minimum required energy in the reactor E_{Req} ’ under the conditions of closed system at which no heat transfer occurs between system boundary.

$$E_{Req} = \Delta H = \sum_{i \in I} n_i H_i(T_2, P_2) - \sum_{i \in I} n_i^F H_i(T_1, P_1) \quad (3.1.1)$$

where, n_i^F and n_i are the number of moles of species i in the feed and product, respectively. Furthermore, $H_i(T_2, P_2)$ and $H_i(T_1, P_1)$ are the specific enthalpies of species i in the feed and product, respectively.

Depending on whether the process is thermodynamically unfavorable ($\Delta G > 0$) or favorable ($\Delta G \leq 0$), the change in energy ΔH can be the minimum energy E_{Req}^{min} required to drive the process or the maximum energy E_{Req}^{max} that can be harnessed from the process. In other words, ΔH becomes the E_{Req}^{min} if chemical species in the feed composition is stable. Carbon dioxide is the most stable chemical species in this reforming model, so the change in enthalpy is supposed to be greater than zero if carbon dioxide is utilized rather than produced. Ideal gas conditions are assumed further.

$$H_i(T, P) = \Delta H_{f,i}^o + \int_{T_o}^T C_p^{ig} dT + H_i^R(T, P) \quad (3.1.2)$$

The enthalpy of a species i can be calculated as above, where $\Delta H_{f,i}^o$ is the standard enthalpy of formation at a reference temperature T_o , C_p^{ig} is the temperature dependent

specific heat capacity in the ideal-gas state, and H_i^R is the residual enthalpy at the current state of species i at T and P . H_i^R supposed to be zero under the ideal gas conditions.

$$H_i(T_1, P_1) = \Delta H_{f,i}^o \quad i \in I \quad (3.1.3)$$

$$H_i(T_2, P_2) = \Delta H_{f,i}^o + \int_{T_1}^{T_2} C_p^{ig} dT = \Delta H_{f,i}^o + R\Phi_i \quad i \in I \quad (3.1.4)$$

Furthermore, because T_0 is equal to T_1 in this work, so enthalpy is expressed as above two equations where Φ_i represents the integral $\int_{T_1}^{T_2} \frac{C_p^{ig}}{R} dT$.

$$\frac{\Delta S_i}{R} = \int_{T_0}^T \frac{C_{p,i}^{ig}}{R} \frac{dT}{T} - \ln \frac{P}{P_0} \quad i \in I \quad (3.1.5)$$

$$S_i^o(T_2, P_2) = S_i^o(T_1, P_1) + R\Psi_i \quad i \in I \quad (3.1.6)$$

The change in Entropy ΔS is expressed as Eq. (3.1.5) and it becomes the Eq. (3.1.6) because P_0 is equal to P in this work, where S_i^o is the standard molar entropy for chemical species i and Ψ_i represents the integral $\int_{T_1}^{T_2} \frac{C_{p,i}^{ig}}{R} \frac{dT}{T}$.

$$C_{p,i}^{ig} = A_i + B_i T + C_i T^2 + D_i T^{-2} \quad i \in I \quad (3.1.7)$$

This equation for $C_{p,i}^{ig}$ is a function of temperature, leading to the following expressions for Φ_i and Ψ_i

$$\Phi_i = A_i T_1 (\tau - 1) + \frac{B_i}{2} T_1^2 (\tau^2 - 1) + \frac{C_i}{3} T_1^3 (\tau^3 - 1) + \frac{D_i}{T_1} \left(\frac{\tau - 1}{\tau} \right) \quad i \in I \quad (3.1.9)$$

$$\Psi_i = A_i \ln \tau + \left[B_i T_1 + \left(C_i T_1^2 + \frac{D_i}{\tau^2 T_1^2} \right) \left(\frac{\tau + 1}{2} \right) \right] (\tau - 1) \quad i \in I \quad (3.1.10)$$

$$\tau = \frac{T_2}{T_1} \quad (3.1.11)$$

3.2 Gibbs Free Energy; Calculation, Regression and Minimization

$\Delta G_{f,i}^o$ is Gibbs free energy of formation at certain temperature and pressure, and can be calculated by linear regression as explained by the supporting information in Appendix A.

$$G_{f,i}^o(T_2, P_2) = G_i^o(T_2, P_2) - \sum_{i \in I_{ref}} G_i^o(T_2, P_2) \quad i \in I \quad (3.2.a1)$$

$$G_i^o(T_2, P_2) = H_i(T_2, P_2) - T_2 * S_i^o(T_2, P_2) \quad i \in I \quad (3.2.a2)$$

Calculation of Gibbs Free Energy of Formation; At equilibrium products at T_2 and P_2 , it is defined as the difference between compound and reference under the assumption of ideal gas and isobaric ($P_1 = P_2 = 1$ bar.) conditions, where I_{ref} is the set of standard elements and species used as reference state, including Carbon (graphite, crystal), Hydrogen (gas), and Oxygen gas.

Although not presented in the above equations, the stoichiometric coefficients in the reaction formula are multiplied inside the sigma at the last term. The coefficients vary by the types of chemical compound ‘ i ’.

$$G_{f,i}^o(T_2, P_2) = \beta_{0,i} + \beta_{1,i}T \quad i \in I \quad (3.2.b1)$$

$$G_{f,i}^o(T_2, P_2) = \beta_{0,i} + \beta_{1,i}T + \beta_{2,i}(T \ln T) + \beta_{3,i}T^2 \quad i \in I \quad (3.2.b2)$$

Moreover, the **Regression** of Gibbs free energy of formation is conducted by the fact that, “for most substances, $G_{f,i}^o(T_2, P_2)$ deviates only slightly from linearity with temperature over a short temperature span” (16) Regression coefficients β are derived from the reference data. Eq. (3.2.b2) is recommended as a formulation of regression, but complicated. Eq. (3.2.b1) is very simple and sufficiently accurate; for example, relative error between formulation and reference data for methane is about 0.1 %.

All Thermodynamics data explained in chapter 3 are organized in Appendix B based on textbook and website (17, 18), including specific heat capacity coefficients, standard enthalpy and Gibbs free energy of formation, standard entropy, and linear regression coefficients of Gibbs free energy.

Gibbs Free Minimization; this is used for the estimation of n_i and n_i^F , both of which are the molar flow rate of each species i , respectively in the reactants and in the equilibrium products at T_2 and P_2 . Specifically, Gibbs energy-based equilibrium criterion is applied for the calculation of n_i , and this criterion is meaning that the total Gibbs energy in the system is most minimized over the nearby-range of temperature, pressure and mixture compositions. Consequently, the terminologies, “minimization, stable, and equilibrium”, are used similar. In addition, n_i^F is simultaneously calculated while the the set of n_i is gained by the Gibbs energy-based equilibrium criterion.

$$G_f^t = \sum_{i \in I} G_{f,i}^o(T_2, P_2) \quad (3.2.c_1)$$

$$\sum_{i \in I} n_i a_{ik} = \sum_{i \in I} n_i^F a_{ik} \quad k \in K \quad (3.2.c_2)$$

$$\sum_k \lambda_k (\sum_{i \in I} n_i a_{ik} - \sum_{i \in I} n_i^F a_{ik}) = 0 \quad (3.2.c_3)$$

The problem is to find the set of n_i 's which minimizes G_f^t for specified T and P, subject to the constraints of the material balances. Lagrange's undetermined multipliers λ_k for each elements are introduced by multiplying each element balance by themselves λ_k .

Sets of n_i^F are usually fixed in typical Gibbs free minimization problem, and summation of atoms in feed molecules is defined as parameter like A_k . However, in this problem, the set of n_i^F is also variable and this makes the consequent formulations more complex than what has been reported in the journals.

$$F = G_f^t + \sum_k \lambda_k (\sum_{i \in I} n_i a_{ik} - \sum_{i \in I} n_i^F a_{ik}) = 0 \quad (3.2.d_1)$$

$$\left(\frac{\partial (n_i a_{ik} - n_i^F a_{ik})}{\partial n_i} \right)_{T,P,n_j} = \left(\frac{\partial n_i}{\partial n_i} \right)_{T,P,n_j^F} - \left(\frac{\partial n_i^F}{\partial n_i} \right)_{T,P,n_j^F} \quad i \in I_{Prod} \quad (3.2.d_2)$$

$$\left(\frac{\partial F}{\partial n_i} \right)_{T,P,n_j} = \left(\frac{\partial G_f^t}{\partial n_i} \right)_{T,P,n_j} + \sum_k \lambda_k \left(1 - \left(\frac{\partial n_i^F}{\partial n_i} \right)_{T,P,n_j^F} \right) a_{ik} = 0 \quad i \in I_{Prod} \quad (3.2.d_3)$$

A new function F is formed by addition of this last sum to G^t , which is identical with G^t because the summation term is zero. However, the partial derivatives of F and G^t with respect to n_i are different, because the function F incorporates the constraints of the material balances.

$$n_i - n_i^F = \sum_r \nu_{i,r} \xi_r \quad i \in I \quad (3.2.e_1)$$

$$\left(\frac{\partial n_i^F}{\partial n_i} \right)_{T,P,n_j} = 1 - \sum_r \nu_{i,r} \left(\frac{\partial \xi_r}{\partial n_i} \right)_{T,P,n_j} \quad i \in I_{Prod} \quad (3.2.e_2)$$

$$\sum_r \nu_{i,r} \left(\frac{\partial \xi_r}{\partial n_i} \right)_{T,P,n_j} = \sum_r \nu_{i,r} * \frac{\Delta \xi_r}{\Delta n_{i,r}} = 1 \quad i \in I_{Prod} \quad (3.2.e_3)$$

$$\Delta n_{i,r} = \nu_{i,r} * \Delta \xi_r \quad i \in I_{Prod}, r \in R \quad (3.2.e_4)$$

The derivation from Eq. (3.2.e₁) to Eq. (3.2.e₄) becomes problematic if $n_i = 0$; however, $n_i \geq 0$ in our model. Technically saying, lower bound of n_i has been already defined bigger than zero because of the logarithm term in Gibbs free minization. Therefore, this formulation is valid, and following equations are showing a simple example to support the previous derivation.

$$\begin{aligned} & \sum_r \nu_{H_2O,r} \left(\frac{\partial \xi_r}{\partial n_{H_2O}} \right)_{T,P,n_j} \\ &= \nu_{H_2O,SMR} * \left(\frac{\Delta \xi_{SMR}}{\Delta n_{H_2O,r}} \right) + \nu_{H_2O,RWGS} * \left(\frac{\Delta \xi_{RWGS}}{\Delta n_{H_2O,r}} \right) + \nu_{H_2O,CBS} * \left(\frac{\Delta \xi_{CBS}}{\Delta n_{H_2O,r}} \right) \end{aligned}$$

$$= \frac{v_{H_2O, SMR} * \Delta \xi_{SMR} + v_{H_2O, RWGS} * \Delta \xi_{RWGS} + v_{H_2O, CBS} * \Delta \xi_{CBS}}{\Delta n_{H_2O, SMR} + \Delta n_{H_2O, RWGS} + \Delta n_{H_2O, CBS}} = 1 \quad (3.2.f_1)$$

$$\because \Delta n_{H_2O, SMR} = v_{H_2O, SMR} * \Delta \xi_{SMR}$$

$$\Delta n_{H_2O, RWGS} = v_{H_2O, RWGS} * \Delta \xi_{RWGS}$$

$$\Delta n_{H_2O, CBS} = v_{H_2O, CBS} * \Delta \xi_{CBS} \quad (3.2.f_2)$$

The formulation with stoichiometric coefficient and extent of reaction is selected, rather than the formulation with n_i^F . Even though both formulations have same meaning, in my head, I picked the former one because considering both reaction pathways i and chemical species r can be more accurate than considering only chemical species i .

$$\left(\frac{\partial G^t}{\partial n_i} \right)_{T,P,n_j} = \mu_i = G_i^\circ + RT \ln \hat{a}_i \quad i \in I_{Prod} \quad (3.2.g_1)$$

$$\mu_i = \Delta G_{f,i}^\circ(T_2, P_2) + RT_2 \ln \frac{n_i}{\sum_{i \in I} n_i} \quad i \in I_{Prod} \quad (3.2.g_2)$$

$$\Delta G_{f,i}^\circ(T_2, P_2) + RT_2 \ln \frac{n_i}{\sum_{i \in I} n_i} + \sum_k \lambda_k \left(\sum_r v_{i,r} \left(\frac{\partial \xi_r}{\partial n_i} \right)_{T,P,n_j} \right) a_{ik} = 0 \quad i \in I_{Prod} \quad (3.2.g_3)$$

$$\Delta G_{f,i}^\circ(T_2, P_2) + RT_2 \ln \frac{n_i}{\sum_{i \in I} n_i} + \sum_k \lambda_k a_{ik} = 0 \quad i \in I_{Prod} \quad (3.2.g_4)$$

The relation between the two equations (3.2.g₁) and (3.2.g₂) is explained in detail at thermodynamic textbooks. (18)

Inside the blanket at the third term of Eq (3.2.g₃) is changed by Eq (3.2.e₃), and the last equation Eq (3.2.g₄) is derived. Eq (3.2.g₄) is satisfied if and only if the products at T_2, P_2 is stable and equilibrium.

The formulation of Gibbs free minimization is not changed between the original equation with feed-mole-parameter and product-mole-variable, and the newly derived equation

with feed-mole-variable and product-mole-variable; however, the newly derived equation requires novel constraints about reaction pathways and extent of reactions as explained in the next subchapter.

3.3 Mole balances and Reaction pathways

$$E_{Req}^{min} = \sum_{i \in I} n_i H_i(T_2, P_2) - \sum_{i \in I} n_i^F H_i(T_1, P_1) \quad (3.3.1)$$

Minimum required energy in the reactor E_{Rct}^{min} is defined as the difference between the enthalpy summation of reactants at T_1, P_1 and the enthalpy summation of equilibrium products at T_2, P_2 . Equation (3.3.1) becomes the objective (O1) in the NLP formulations as explained in the next section. Physical meaning of minimum required energy objective (O1) is ensured by Material balance constraint and Gibbs free minimization constraint. In other words, co-working with two constraints, elements conservation and chemical stability are assured accurately without violating actual physical phenomenon. This has been reported and applied several times in the journal. However, in order to explore the thermodynamic limits, minimum required energy has to be calculated through improving the constraints with stoichiometric coefficients $\nu_{i,r}$ and extent of reaction ξ_r .

$$n_i - n_i^F = \sum_r \nu_{i,r} \xi_r \quad i \in I \quad (3.3.2)$$

$$\xi_r = 0 \quad \forall r \in \{R \setminus R_{rct}\} \quad r \in R \quad (3.3.3)$$

Reactors by reactors, numerically so many reaction pathways ‘r’ can be occurred among the chemical species. Some part of the whole reaction pathways ‘r’ is classified as valid pathways of reactor R_{rct} . Only these valid reaction pathways ‘ R_{rct} ’ are related with the research topics, and the others stray from the subject. Therefore, the equation (3.3.3)

makes the extent of the reaction ξ_r , which are assigned to digressed reaction pathways, having zero value. Subset R_{rct} has to be carefully confirmed based on reaction kinetics and empirical data as explained in this subchapter. Even though two equations are well known and explained in thermodynamic textbook, they have not been applied to the process intensification of CO₂ utilization.

Reaction pathways ‘ r ’ and their ξ_r in the syngas production model are showed as a good example to derive the equations step by step, also supporting necessity of them.



In the syngas production model, chemical species set ‘ i ’ are composed of 6 molecules; methane, carbon dioxide, carbon monoxide, hydrogen, oxygen, and water. Therefore, 8 reaction pathways, related with these chemical species, can be occurred as the syngas-production-alternatives and/or CO₂ utilization. Code names are assigned right to reaction pathways r (formulations). $RS(r)$ is the subset of reaction pathways r related with syngas production.

$$\xi_{\text{RS } 1} = \frac{n_{\text{CH}_4} - n_{\text{CH}_4}^F}{-1} = \frac{n_{\text{CO}_2} - n_{\text{CO}_2}^F}{-1} = \frac{n_{\text{CO}} - n_{\text{CO}}^F}{2} = \frac{n_{\text{H}_2} - n_{\text{H}_2}^F}{2} \quad (3.3.a_1)$$

$$\xi_{\text{RS } 2} = \frac{n_{\text{CH}_4} - n_{\text{CH}_4}^F}{-1} = \frac{n_{\text{O}_2} - n_{\text{O}_2}^F}{-0.5} = \frac{n_{\text{CO}} - n_{\text{CO}}^F}{1} = \frac{n_{\text{H}_2} - n_{\text{H}_2}^F}{2} \quad (3.3.a_2)$$

$$\xi_{\text{RS } 3} = \frac{n_{\text{CH}_4} - n_{\text{CH}_4}^F}{-1} = \frac{n_{\text{H}_2\text{O}} - n_{\text{H}_2\text{O}}^F}{-1} = \frac{n_{\text{CO}} - n_{\text{CO}}^F}{1} = \frac{n_{\text{H}_2} - n_{\text{H}_2}^F}{3} \quad (3.3.a_3)$$

$$\xi_{RS4} = \frac{n_{CO_2} - n_{CO_2}^F}{-1} = \frac{n_{H_2} - n_{H_2}^F}{-1} = \frac{n_{CO} - n_{CO}^F}{1} = \frac{n_{H_2O} - n_{H_2O}^F}{1} \quad (3.3.a4)$$

$$\xi_{RS5} = \frac{n_{CH_4} - n_{CH_4}^F}{-1} = \frac{n_{O_2} - n_{O_2}^F}{-1} = \frac{n_{CO_2} - n_{CO_2}^F}{1} = \frac{n_{H_2} - n_{H_2}^F}{2} \quad (3.3.a5)$$

$$\xi_{RS6} = \frac{n_{CH_4} - n_{CH_4}^F}{-1} = \frac{n_{O_2} - n_{O_2}^F}{-2} = \frac{n_{CO_2} - n_{CO_2}^F}{1} = \frac{n_{H_2O} - n_{H_2O}^F}{2} \quad (3.3.a6)$$

$$\xi_{RS7} = \frac{n_{CH_4} - n_{CH_4}^F}{-1} = \frac{n_{H_2O} - n_{H_2O}^F}{-2} = \frac{n_{CO_2} - n_{CO_2}^F}{1} = \frac{n_{H_2} - n_{H_2}^F}{4} \quad (3.3.a7)$$

$$\xi_{RS8} = \frac{n_{CO} - n_{CO}^F}{-1} = \frac{n_{H_2O} - n_{H_2O}^F}{-1} = \frac{n_{CO_2} - n_{CO_2}^F}{1} = \frac{n_{H_2} - n_{H_2}^F}{1} \quad (3.3.a8)$$

ξ_r , an extent of reaction, is defined as $\xi_r = \frac{\Delta n_i}{v_{i,r}} = \frac{n_{equilibrium} - n_{initial}}{v_{i,r}}$, where $v_{i,r}$ is stoichiometric coefficient of chemical species i in reaction pathways r . Below equations ξ_r can be expressed when only one reaction pathway r goes and the others don't.

$$n_{CH_4} - n_{CH_4}^F = -\xi_{RP1} - \xi_{RP2} - \xi_{RP3} - \xi_{RP5} - \xi_{RP6} - \xi_{RP7} \quad (3.3.b1)$$

$$n_{CO_2} - n_{CO_2}^F = -\xi_{RP1} - \xi_{RP4} + \xi_{RP5} + \xi_{RP6} + \xi_{RP7} + \xi_{RP8} \quad (3.3.b2)$$

$$n_{CO} - n_{CO}^F = 2 * \xi_{RP1} + \xi_{RP2} + \xi_{RP3} + \xi_{RP4} - \xi_{RP8} \quad (3.3.b3)$$

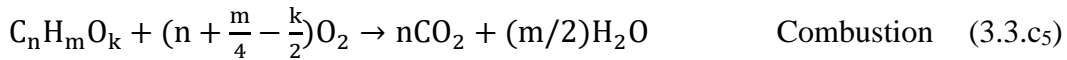
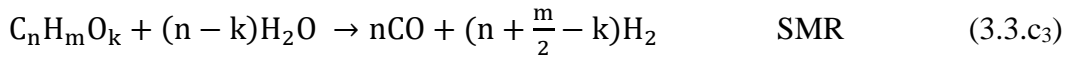
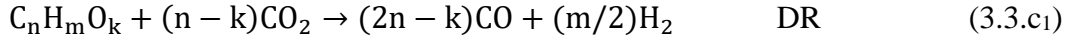
$$n_{H_2} - n_{H_2}^F = 2\xi_{RP1} + 2\xi_{RP2} + 3\xi_{RP3} - \xi_{RP4} + 2 * \xi_{RP5} + 4 * \xi_{RP7} + \xi_{RP8} \quad (3.3.b4)$$

$$n_{H_2O} - n_{H_2O}^F = -\xi_{RP3} + \xi_{RP4} + 2 * \xi_{RP6} - 2 * \xi_{RP7} - \xi_{RP8} \quad (3.3.b5)$$

$$n_{O_2} - n_{O_2}^F = -0.5 * \xi_{RP2} - \xi_{RP5} - 2 * \xi_{RP6} \quad (3.3.b6)$$

All types of reaction pathway can occur, rather than one, in real reactor. Therefore, difference of moles between product and feed at each chemical species is expressed through summing the stoichiometric coefficients timed by extent of reactions.

Instead of focusing methane and expressing reaction formulas like from RP 01 to RP 08, generalized reaction formulas of hydrocarbons $C_nH_mO_k$ are more convenient when chemical model to be modified for extensive study.



Zero or positive value can be assigned to ξ_r , depending on what types of reaction pathways ' r ' are desirable or realistic. (RS 5) & (RS 6) & (RS 7) & (RS 8) can be controversial because these reaction pathways are producing carbon dioxide, rather than utilizing it. For example, in the case of oxygen-related reaction pathways, combustion is unwanted reaction type but can be happened in the realistic reactor. The information about the ratio of the degree of combustion reaction to the degree of partial oxidation reaction at the given reactor conditions is used so as to set below constraint if T_2 is over 1073 K and feed composition oxygen per hydrocarbon is less than 0.5. (19)

$$\xi_{\text{Combustion}}/\xi_{\text{Partial Oxidation}} \leq 0.02 \quad (3.3.c_6)$$

Interestingly, even if $\xi_{\text{Combustion}}$ is set to 0 and the above constraint is excluded, reactors are satisfied the conditions of high temperature and low oxygen-hydrocarbon composition. This is because combustion is very exothermic and needs large moles of oxygen, so equilibrium products simulated by GAMS favors high temperature and low oxygen ratio.

Less combustion is desirable in this chemical model of which the objective variables are to obtain minimum requirement energy for reforming alternatives and CO₂ utilization.

Likewise, based on reaction kinetics, CO₂-utilizing reactions favor high temperature and have high reaction constant while CO₂-consuming reactions are inverse. Therefore, it is reasonable to assign zero or very low value to CO₂-consuming reactions.

If the CO₂-producing reactions are not constrained, the mole balance constraint are unnecessary. In other words, there is no need to control the chemical model reaction by reaction. However, if not constrained, CO₂-producing reactions are able to have large value, which makes the minimum requirement energy of oxygen-related reactor become very negative, not to mention that this values are matched with the reaction enthalpy of combustion.

$$n_i - n_i^F = \sum_r \nu_{i,r} \xi_r \quad i \in I \quad (3.3.2)$$

Again, for the above reasons, mole balance constraint with the extent of reaction is essential. Precise value of minimum requirement energy can be acquired by mole balance equations with adequate reaction pathways. With these equations, positive value is obtained and well-matched by the means of the utilization of very stable chemical species CO₂.

3.4 Objective Variables

Minimum Required Energy “the minimum energy equals to the minimum work that must be done to separate a mixture into its pure components which is equal to the changes in Gibbs free energy of a reversible process.” (8)

$$E_{Req} = \sum_{i \in I} n_i H_i(T_2, P_2) - \sum_{i \in I} n_i^F H_i(T_1, P_1) \quad (3.4.1)$$

Separation Energy E_{Sep} is the theoretical minimum work required to completely separate syngas from the ideal product mixture. This can be obtained by calculating the Gibbs free energy change of mixing ΔG_{mix} under the conditions of a reversible isothermal, isobaric change.

$$E_{Sep} = \Delta G_{mix} = -T \Delta S_{mix} = - \sum_{i \in I} n_i RT (x_1 \ln x_1 + x_2 \ln x_2) \quad (3.4.2)$$

, where

$$x_1 = \frac{n_{H_2} + n_{CO}}{\sum_{i \in I} n_i}, \quad x_2 = \frac{\sum_{i \in I} n_i - (n_{H_2} + n_{CO})}{\sum_{i \in I} n_i} \quad (3.4.3)$$

Therefore, the same NLP model can be used to calculate the minimum energy for combined production and separation of H₂ and CO as pure syngas. The only modification that is needed is the revision of the objective function as follows:

$$\min_{T_2, n_i^F} E_{Req} = \sum_{i \in I} n_i H_i(T_2, P_2) - \sum_{i \in I} n_i^F H_i(T_1, P_1) + E_{Sep} \quad (3.4.4)$$

Carbon Dioxide Utilization Since the ultimate purpose of the process is to utilize CO₂ to produce syngas, it is important that we calculate the net CO₂ conversion which is calculated by subtracting the unreacted CO₂ (n_{CO_2}) and the auxiliary CO₂ emission ($n_{CO_2}^{aux}$) from the total CO₂ fed to the system ($n_{CO_2}^F$). (8)

$$n_{CO_2}^F - n_{CO_2} - n_{CO_2}^{aux} = U_{CO_2} n_{CO_2}^F \quad (3.4.5)$$

$$n_{CO_2}^F = 1; n_i^F = 0 \quad \forall i \in \{I \setminus I_F\} \quad (3.4.6)$$

$$n_{CO_2}^{aux} = \phi E_{Req} \quad (3.4.7)$$

Eq. (3.4.5) calculates Carbon Dioxide Utilization U_{CO_2} , and $n_{CO_2}^F$ is fixed to one so as to normalize the calculation as shown in Eq. (3.4.6). Furthermore, because subset I_F for chemical species of feed is changed depending on the reactor types such as PODR, CDSR, and CR, Eq. (3.4.6) shows that the number of moles is fixed to zero for some species which are not present in the feed.

The auxiliary CO₂ emission is calculated using Eq. C10, which is constant emission factor φ multiplied by the energy required by the system (E_{Req}). In this work, auxiliary emission is assumed as a linear function of the energy utilized in a system.

Syngas Selectivity In order to obtain the maximum syngas ($H_2 + CO$) selectivity S_{SG} in the equilibrium product mixture, new objective function is given as follows

$$n_{H_2} + n_{CO} = S_{SG} \sum_{i \in I_{Prod}} n_i \quad (3.4.8)$$

3.5 Coke-deposition; Reaction Kinetics and Gibbs Free Minimization

In this subchapter, reaction kinetics and thermodynamic formulations are discussed. Followings are reactions pathways in coke-deposition and coke-removal.



Reaction Kinetics Reaction rate of Boudouard Reaction is lowered a factor of 20 in the presence of hydrogen, compared with the absence of hydrogen. Reaction order of

hydrogen at the Boudouard reaction is well known, which is the second-order inverse. Once coke formation initiated, this rate tends to keep remain even with the high syngas ratio. (20)

Presence of Hydrogen also suppresses the reaction of hydrocarbon decomposition into coke. Activation energy of hydrocarbon decomposition is very high in the paraffin at most, compared to olefins and acetylenes. Reaction rate of Hydrocarbon decomposition is minimized at 600 deg C, and increases in the increase of temperature. Presence of steam removes the coke, and generating carbon monoxide and hydrogen. (20)

Gibbs Free Minimization Following constraints are required to describe the equilibrium products with coke.

$$n_{Coke} = 10^{-10} \quad (3.5.6)$$

$$\sum_{i \in I_{Gas}} n_i * \left[\Delta G_{f,i}^o(T_2, P_2) + RT_2 \ln \frac{n_i}{\sum_{i \in I_{Gas}} n_i} + \sum_k \lambda_k a_{ik} \right] + n_{Coke} * \Delta G_{f,Coke}^o(T_2, P_2) = 0 \quad (3.5.7)$$

Eq. (3.5.6) is valid under the assumption of free-coke deposition, and Eq. 3.5.7 is referenced from the article (21)

3.6 Nonlinear (NLP) Optimization Model

NLP optimization model has been developed to calculate the thermodynamically minimum energy in the syngas production system with H₂:CO ratio specification. This model is based on the ‘Enthalpy and Entropy Calculation’ and ‘Gibbs Free Minimization’. The complete formulation of the NLP model is provided below.

Sets and Indices

- i chemical species ($i \in I$, I is the set of total species in the system)
- k chemical element ($k \in K$, where K is the set of total elements)
- r reaction pathways ($r \in R$, where R is the set of total reaction pathways)

* Subsets $I_{Ref}(i)$, $IB(i)$, $I_{Feed}(i)$, $I_{Prod}(i)$, and $R_{rct}(r)$ are explained in Appendix A.

Parameters:

- T_1, P_1 Initial feed temperature and pressure
- $\Delta G_{f,i}^o, \Delta H_{f,i}^o$ Gibbs free energy of formation and Enthalpy of formation at T_1 and P_1
for chemical species i under standard condition
- R^{ig} Ideal gas constant
- a_{ik} number of atoms of the k th element in chemical species i
- r_{SG} ratio of H₂ and CO moles in the product syngas
- A_i, B_i, C_i, D_i Heat capacity coefficients of chemical species for ideal gas
- $\nu_{i,r}$ Stoichiometric coefficients of chemical species i in reaction pathways r
- $\beta_{0,i}, \beta_{1,i}$ Regression coefficients for Gibbs free energy of formation.
- T_2^L, T_2^U Lower and upper bound of the final temperature (= 300 K, 1500 K)
- P_2^L, P_2^U Lower and upper bound of the pressure (= 1bar)
- $n_i^{F,L}, n_i^{F,U}$ Lower and upper bounds of molar feed variables (= 0.001 mol, 1000 mol)
- n_i^L Lower bound of molar equilibrium product variables
(=Inverse of Avodadro's Number = $(6.022 \cdot 10^{23})^{-1}$)

Variables:

- E_{Req} Minimum required energy for reactors.

S_{SG}	Minimum combined H ₂ and CO selectivity over other species in syngas
U_{CO_2}	Fraction of CO ₂ from the feed that must be converted
T_2, P_2	Product temperature and pressure
$\Delta G_{f,i}^o(T_2, P_2), H_i(T_2, P_2)$	Gibbs free energy of formation and Enthalpy of formation at equilibrium products T_2 and P_2 for chemical species i under standard condition
n_i, n_i^F	Number of moles of chemical species i in the feed and in the equilibrium products at T_2 and P_2
Φ_i	Integration of sensible heat for chemical species i over temperature span.
$n_{CO_2}^{aux}$	Auxiliary emission (moles of CO ₂) to supply energy for the system
φ	Auxiliary emission calculation.
λ_k	Lagrange multiplier corresponding to material balance for k th element
ξ_r	Extent of reaction with respect to realistic reaction pathways r .

NLP Model Formulation

$$\min_{T_2, n_i^F} E_{Req},$$

, where

$$E_{Req} = \sum_{i \in I} n_i H_i(T_2, P_2) - \sum_{i \in I} n_i^F H_i(T_1, P_1) + E_{Sep} \quad (O1)$$

$$n_{CO_2}^F - n_{CO_2} - n_{CO_2}^{aux} = n_{CO_2}^F U_{CO_2} \quad (O2)$$

$$n_{H_2} + n_{CO} = S_{SG} \sum_{i \in I_{Prod}} n_i \quad (O3)$$

Subject to

$$H_i(T_1, P_1) = \Delta H_{f,i}^o \quad (C1)$$

$$H_i(T_2, P_2) = \Delta H_{f,i}^o + \int_{T_1}^{T_2} C_p^{ig} dT = \Delta H_{f,i}^o + R\Phi_i \quad (C2)$$

$$\Delta G_{f,i}^o(T_2, P_2) + RT_2 \ln \frac{n_i}{\sum_{i \in I_{Gas}} n_i} + \sum_k \lambda_k a_{ik} = 0 \quad i \in I_{Prod} \quad (C3)$$

$$\Delta G_{f,i}^o(T_2, P_2) = \beta_{0,i} + \beta_{1,i} T_2 \quad i \in I_{Prod} \quad (C4)$$

$$\sum_{i \in I} n_i a_{ik} = \sum_{i \in I} n_i^F a_{ik} \quad k \in K \quad (C5)$$

$$\Phi_i = A_i T_1 (\tau - 1) + \frac{B_i}{2} T_1^2 (\tau^2 - 1) + \frac{C_i}{3} T_1^3 (\tau^3 - 1) + \frac{D_i}{T_1} \left(\frac{\tau - 1}{\tau} \right) \quad i \in I_{Prod} \quad (C6)$$

$$n_{Coke} = 10^{-10} \quad (C7)$$

$$\sum_{i \in I_{Gas}} n_i * \left[\Delta G_{f,i}^o(T_2, P_2) + RT_2 \ln \frac{n_i}{\sum_{i \in I_{Gas}} n_i} + \sum_k \lambda_k a_{ik} \right] + n_{Coke} * \Delta G_{f,Coke}^o(T_2, P_2) = 0 \quad (C8)$$

$$\tau = \frac{T_2}{T_1} \quad (C9)$$

$$n_{H_2} = r_{SG} n_{CO} \quad (C10)$$

$$n_{CO_2}^F = 1; n_i^F = 0 \forall i \in \{I \setminus I_F\} \quad (C11)$$

$$n_{CO_2}^{aux} = \varphi E_{Req} \quad (C12)$$

$$T_2^L \leq T_2 \leq T_2^U, P_2^L \leq P_2 \leq P_2^U, n_i^{F,L} \leq n_i^F \leq n_i^{F,U} \quad (C13)$$

$$n_i - n_i^F = \sum_r \nu_{i,r} * \xi_r \quad i \in I_{Prod} \quad (C14)$$

Solver for NLP model; ANTIGONE (22)

To make sure the GAMS results are global optimal with solver ANTIGONE, some variables are highly recommended to be re-scaled as follows;

$$G_{f,i}^o(T_2, P_2) + RT_2 * \left\{ \ln \left(e^{15} * \frac{n_i}{\sum_{i \in I_{Gas}} n_i} \right) - 15 \right\} + \sum_k \lambda_k a_{ik} = 0 \quad i \in I_{Prod} \quad (3.6.1)$$

$$n_{CO_2}^F - n_{CO_2} - n_{CO_2}^{aux} = n_{CO_2}^F (0.01 * U_{CO_2}) \quad (3.6.2)$$

$$n_{H_2} + n_{CO} = (0.01 * S_{SG}) \sum_{i \in I_{Prod}} n_i \quad (3.6.3)$$

$U_{CO_2}^L$ lower bound of carbon utilization is required because the energy requirement and the carbon utilization are trade-offs for each other. Either one of following two equations are used, and numerical numbers here can be adjusted. Eq. (3.6.5) is based on Eq. (3.3.c6)

$$U_{CO_2}^L = 50 (\%) \quad (3.6.4)$$

$$\xi_{Combustion} / \xi_{Partial Oxidation} \leq 0.02 \quad (3.6.5)$$

3.7 Results for CO₂ Utilization and Methane Reforming at Equilibrium Conditions

Preliminary work (8) lacks or incorrectly describes followings; Calculation of Gibbs Free Energy, normalization of Objective values, derivation of Gibbs free minimization with feed variables, and mole balances with extent of reactions. Figure 3.2 is improved from the preliminary work, so as to theoretically describe the chemical reaction exactly based on chapter 3.1 ~3.6.

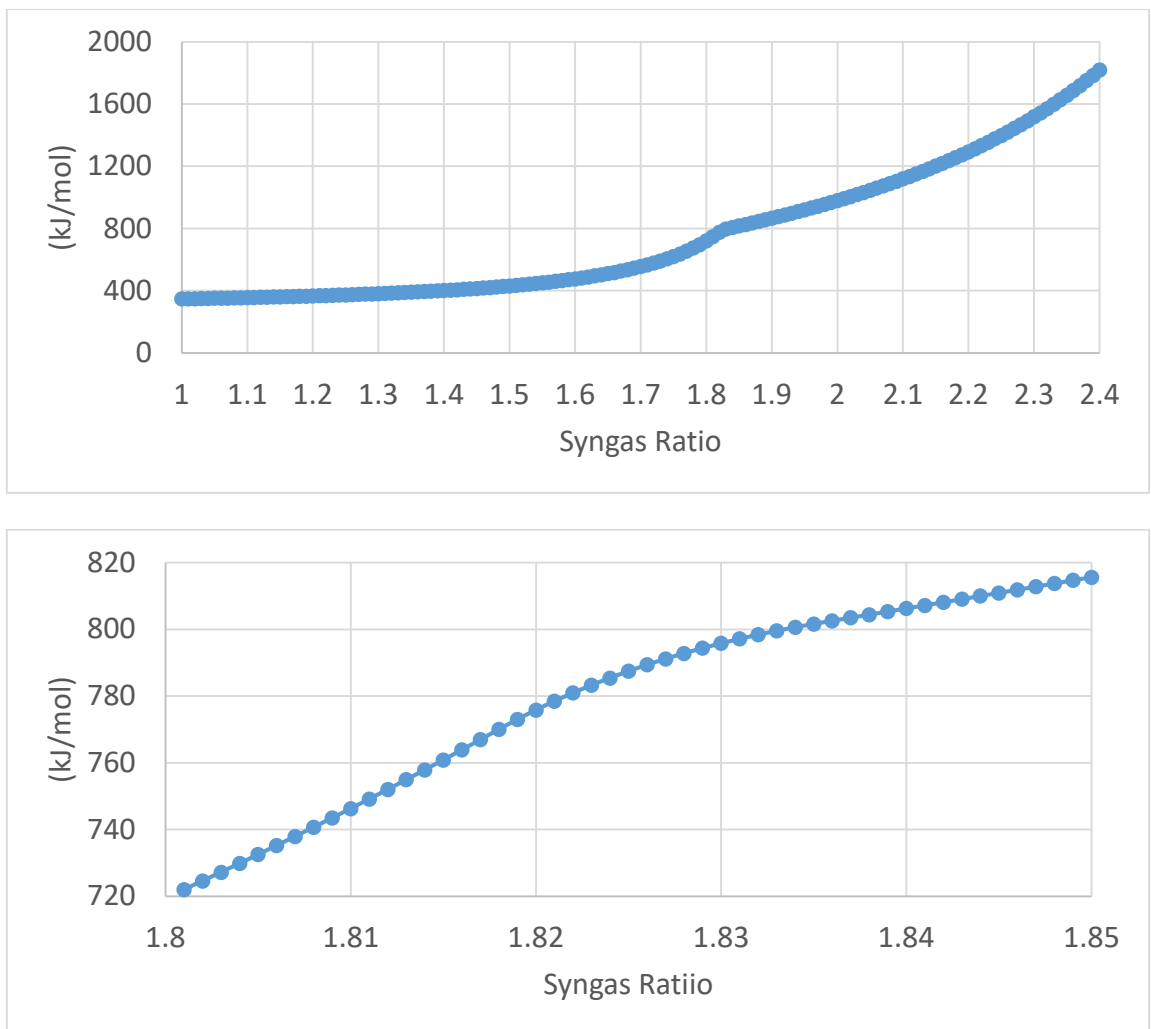
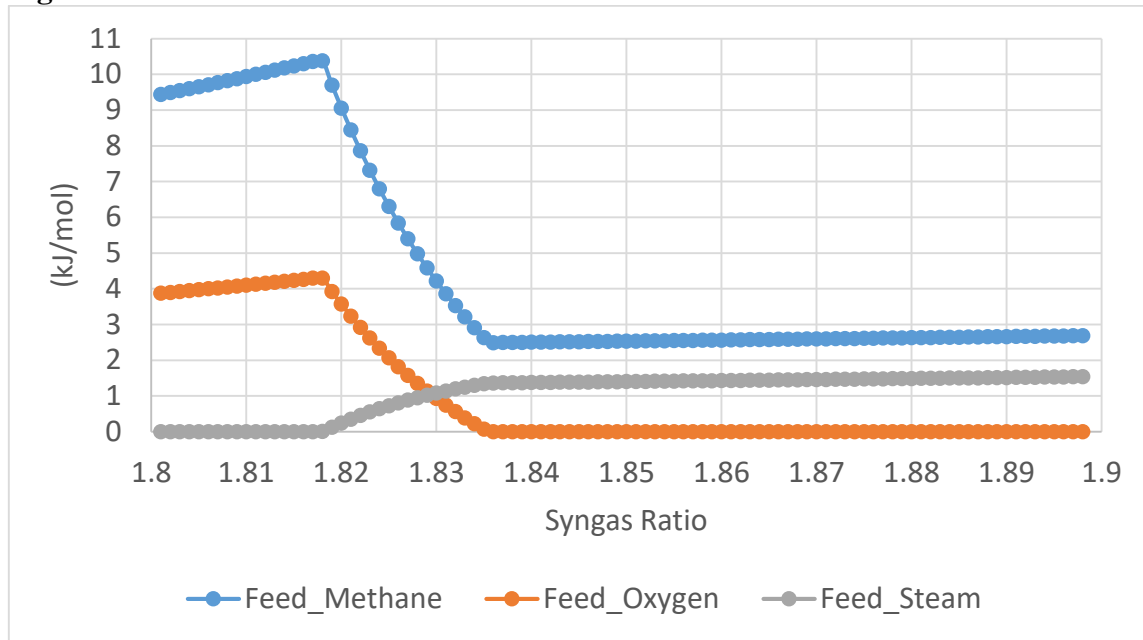


Figure 3 Results from the energetic analysis for syngas production.

Figure 3 Continued



Syngas Ratio	Model Objective	Article Information (Kinetic Modeling)	
		1.3	380 kJ/mole
1.5	430 kJ/mole	423.1 kJ/mole, $U_{CO_2} = 65 \%$	Challiwala et al (2016)
2.0	979 kJ/mole	Unknown Energy, $U_{CO_2} > 90 \%$	Zhang et al (2014)

(From up to down) ^{1), 2)} Thermodynamically minimum energy requirement (kJ) per CO₂ utilization (moles) ³⁾ Feed Composition. ⁴⁾ Rough Comparison with Articles. CO₂ utilization constraint is fixed as 90 % (0.9 mole), and the lower bound of feed composition is 10⁻⁶ (mole).

Energy-requirement curves (kJ/mol) with respect to syngas ratio are shown in the first two figures. It seems like that breaking point appeared at the range of syngas ratio between 1.82 and 1.83; however, this curve is proved to be intrinsically smooth, supported by the

enlarged figure with syngas ratio from 1.80 to 1.85. No other breaking point appears, supported by zooming the curve in.

In the range of syngas ratio between 1.818 to 1.836, the feed composition is changed dramatically; feed mole of steam is increased as syngas ratio become large, and feed mole of oxygen is decreased to the lower bound. These changes are explained by the reforming types; steam is required for producing the high syngas ratio and oxygen for low syngas ratio. In addition, syngas ratio lower than 1.818, the feed moles of methane and oxygen are going down, because the porting of dry reforming is on increase rather than partial oxidation of methane.

According to the 'Table 2-2 Energy generation per CO₂ emission in regard to primary energy resources', at the syngas ratio of 2 the energy requirement per CO₂ utilization is larger than the combustion energy of natural gas. In other words, carbon utilization via methane reforming at syngas ratio of 2 is indirectly emitting the CO₂ more than the CO₂ utilized. In same regard, it can be stated that combined reformers of methane are able to contribute to CO₂ utilization lower than the syngas ratio of 1.91.

The difference between the objective variables from the current model and articles is observed. This is because model developments are different; the current model is based on chemical equilibrium and ideal-gas state whereas articles are based on kinetic modeling. This rough comparison can be used as supplementary information to check whether or not thermodynamics equations are correct.

Most frequent value of final temperature T_2 are occurred between 1073 K ~ 1211 K, and the highest value is 1211 K. The temperature values lower than 1073 K appear

occasionally. Generally saying, high syngas ratio at which steam reforming is dominant requires high temperature because of high endothermic reaction enthalpy.

CHAPTER IV

EXTENSIVE STUDIES FOR METHANOL AND ETHANE

4.1 Novel Constraints for Gas Sepataion and Methanol Synthesis

Followings are added to the previous model discussed in chapter 3.

Set;

n_i^R Chemical species feed into combined methane reforming reactor.

n_i^R Chemical species at equilibrium products from the reforming reactor.

n_i^{Rin} Subgroup of n_i^R where $y_i = 1$.

n_i^M Chemical species at equilibrium products from the methanol synthesis reactor.

Parameter;

N_A Avogadro's Number. M Large number (e.g. 10^6)

Variable;

y_i Binary variable for determining air separation

$y_i = 0$ for the species separated out.

$y_i = 1$ for the species included in the equilbirum products.

E_{req}^R Enthalpy Difference between Feed n_i^F and Reformed species $n_i^R + E^{Separation}$

E_{req}^M Enthalpy Difference between n_i^{R-in} and Methanol Products $n_i^M + E^{Compression}$

Objective;

To minimize $E_{req}^{Overall} = \sum_{i \in I} y_i n_i^M H_i(T_3, P_3) + \sum_{i \in I} (1 - y_i) n_i^R H_i(T_2, P_2) -$

$\sum_{i \in I} n_i^F H_i(T_1, P_1) - n_{sum}^R RT(x_1 \ln x_1 + x_2 \ln x_2) + n_{sum}^{R-in} R^{IG} \ln(P_2/P_1)$

$$, \text{where } n_{sum}^R = \sum_{i \in I} n_i^R \quad n_{sum}^{R.in} = \sum_{i \in I} y_i n_i^R$$

$$x_1 = \frac{\sum_{i \in I} y_i n_i^R}{\sum_{i \in I} n_i^R} \quad x_2 = \frac{\sum_{i \in I} (1-y_i) n_i^R}{\sum_{i \in I} n_i^R} \quad (4.1.O)$$

Subject to;

$$\sum_{i \in I_M} n_i^R a_{ik} = \sum_{i \in I_M} n_i^M a_{ik} \quad k \in K \quad (4.1.C1)$$

$$y_i * \left[\Delta G_{f,i}^o(T_3, P_3) + RT_3 \ln \frac{(1/N_A)^{+y_i n_i^M}}{\sum_{i \in I} n_i^M} + \sum_k \lambda_k^M a_{ik} \right] = 0 \quad i \in I_M \quad (4.1.C2)$$

$$0 \leq M * y_i - n_i^M < M \quad i \in I_M \quad (4.1.C3)$$

4.2 Novel Constraints for Linear Dependence of Reacton Pathways

Unlike in the methane tri-reforming where the number of constraints are sufficient to describe the reaction pathways, new constraints derived from the linear dependence of reaction pathways are required for ethane tri-reforming. As belows, there are 20 realistic reactions pathways in ethane tri-reforming, and all these extent of reactions are variables.

- (1) $\text{CH}_4 + \text{CO}_2 \rightarrow 2\text{CO} + 2\text{H}_2$
- (2) $\text{CH}_4 + \frac{1}{2}\text{O}_2 \rightarrow \text{CO} + 2\text{H}_2$
- (3) $\text{CH}_4 + \text{H}_2\text{O} \rightarrow \text{CO} + 3\text{H}_2$
- (4) $\text{CO}_2 + \text{H}_2 \rightarrow \text{CO} + \text{H}_2\text{O}$
- (5) $\text{CH}_4 + 2\text{O}_2 \rightarrow \text{CO}_2 + 2\text{H}_2\text{O}$
- (6) $\text{CH}_4 \rightarrow \text{C} + 2\text{H}_2$
- (7) $2\text{CO} \rightarrow \text{C} + \text{CO}_2$
- (8) $\text{C} + \text{CO}_2 \rightarrow 2\text{CO}$
- (9) $\text{C} + \text{H}_2\text{O} \rightarrow \text{CO} + \text{H}_2$
- (10) $\text{C} + \text{O}_2 \rightarrow \text{CO}_2$
- (11) $\text{C}_2\text{H}_6 + 2\text{CO}_2 \rightarrow 4\text{CO} + 3\text{H}_2$
- (12) $\text{C}_2\text{H}_6 + \text{CO}_2 \rightarrow \text{CH}_4 + 2\text{CO} + \text{H}_2$
- (13) $\text{C}_2\text{H}_6 + \frac{7}{2}\text{O}_2 \rightarrow 2\text{CO}_2 + 3\text{H}_2\text{O}$
- (14) $\text{C}_2\text{H}_6 + \text{O}_2 \rightarrow 2\text{CO} + 3\text{H}_2$
- (15) $\text{C}_2\text{H}_6 + \frac{1}{2}\text{O}_2 \rightarrow \text{CH}_4 + \text{CO} + \text{H}_2$
- (16) $\text{C}_2\text{H}_6 + 2\text{H}_2\text{O} \rightarrow 2\text{CO} + 5\text{H}_2$
- (17) $\text{C}_2\text{H}_6 + \text{H}_2\text{O} \rightarrow \text{CH}_4 + \text{CO} + 2\text{H}_2$
- (18) $\text{C}_2\text{H}_6 \rightarrow 2\text{C} + 3\text{H}_2$
- (19) $\text{C}_2\text{H}_6 \rightarrow \text{C}_2\text{H}_4 + \text{H}_2$
- (20) $2\text{H}_2 + \text{O}_2 \rightarrow 2\text{H}_2\text{O}$

Figure 4 Realistic reaction pathways in ethane tri-reforming.

Following instructions are added to the previous model discussed in chapter 3, and explanation for constraints are followed step by step.

Indices and set;

ld (indice) Indicating combinations which make linear dependence

R_{Main} (set) Subgroup for essential reaction pathways which should be independent

Parameter;

$ST_{r,i}^{Matrix}$ Matrix for stoichiometric coefficients in ethane tri-reforming.

M Large number (e.g. 10^6)

Variable;

$C_{r,ld}$ Combinations which make linear dependence ld of reaction pathways r

$B_{r,ld}$ Binary variable for $C_{r,ld}$

$B''_{r,ld}$ Binary variable for ensuring the uniqueness of $B_{r,ld}$

Explanation for constraints;

$$\sum_r ST_{r,i}^{Matrix} * C_{r,ld} = 0 \quad \text{for } i \in I, \text{ for } ld \in LD \quad (4.2.a_1)$$

$$-1 \leq C_{r,ld} \leq 1 \quad \text{for } rt \in RT, \text{ for } ld \in LD \quad (4.2.a_2)$$

$$0 \leq M * B_{r,ld} - C_{r,ld}^2 < M \quad \text{for } rt \in RT, \text{ for } ld \in LD \quad (4.2.a_3)$$

$$2 \leq \sum_r B_{r,ld} \leq card(r) - rank(ST_{r,i}^{Matrix}) \quad \text{for } ld \in LD \quad (4.2.a_4)$$

Eq. (4.2.a2) is for upper and lower bounds, and Eq. (4.2.a4) is meaning that the number of element in the vector is at least 2 and at most the number of dependent vectors in $ST_{r,i}^{Matrix}$. (The function $card$ calculates the number of elements in certain set, and the function $rank$ calculates the the number of independent vectors in certain matrix.)

$$R_{Main} = \{CH_4Dry, CH_4Pox, CH_4Steam, CH_4Cracking, GasificationCO_2, GasificationH_2O\} \quad (4.2.a5)$$

$$R_{Main} = \{C_2H_6Dry, C_2H_6Pox, C_2H_6Steam, C_2H_6Cracking, GasificationCO_2, GasificationH_2O\} \quad (4.2.a6)$$

$$\sum_r B_{r,ld} \geq 1 \quad \text{if } r \in \{R/R_{Main}\} \quad (4.2.a7)$$

R_{Main} is the subset of reaction pathways, which should be intrinsically independent. In other words, there is no $C_{rt,ld}$ column that makes the linear dependence inside R_{Main} subset. R_{Main} is composed of 3 reforming reactions, 1 cracking reaction, and 2 gasification reactions. The reaction gasification by CO_2 can be replaced by Boudouard reaction, but selected in R_{Main} in order to include more coke-removing reactions. The reaction gasification by steam is selected because very effective for removing coke better than the other gasification reactions. (20)

Eq. (4.2.a5) and Eq. (4.2.a6) are representing the main reaction pathways of methane tri-reforming and ethane tri-reforming, respectively. Eq. (4.2.a7) is meaning that every combination for linear dependence must contain at least one reaction pathway except for R_{Main} .

$$(B_{r,ld} - B_{r,ld'})^2 \leq B''_{r,ld} \leq B_{r,ld} + B_{r,ld'} \quad \text{for } r \in R, \text{ for } ld \in LD, \text{ for } ld' \in LD \quad (4.2.b1)$$

$$B''_{r,ld} \leq 2 - (B_{r,ld} + B_{r,ld'}) \quad \text{for } r \in R, \text{ for } ld \in LD, \text{ for } ld' \in LD \quad (4.2.b2)$$

$$\sum_r (B_{r,ld} + B''_{r,ld} - B_{r,ld'}) \neq 0$$

$$\text{for } ld \in LD, \text{ for } ld' \in LD, \text{ when } ord(ld) \neq ord(ld') \quad (4.2.b_3)$$

$$\sum_{rt} (B_{r,ld} + B''_{r,ld} - B_{r,ld'}) = 0$$

$$\text{for } ld \in LD, \text{ for } ld' \in LD, \text{ when } ord(ld) = ord(ld') \quad (4.2.b_4)$$

$$\sum_r B_{r,ld} = A_{ld} \quad \text{for } ld \in LD \quad (4.2.b_5)$$

Above equations from Eq. (4.2.b1) to Eq. (4.2.b4) are for ensuring the uniqueness of $B_{r,ld'}$, and A_{ld} is used as objective. Followings are summations of simple columns to validate the equations. If the column summation is equal to null vector (zero vector), then redundancy between the two columns is proved. Else, uniqueness is ensured.

Case1; when $B_{r,ld} = \{1 \ 0 \ 0\}$ and $B_{r,ld'} = \{1 \ 1 \ 0\}$

$$\begin{pmatrix} 1 \\ 0 \\ 0 \end{pmatrix} + \begin{pmatrix} 0 \\ 1 \\ 0 \end{pmatrix} - \begin{pmatrix} 1 \\ 1 \\ 0 \end{pmatrix} = \begin{pmatrix} 0 \\ 0 \\ 0 \end{pmatrix} \quad \begin{pmatrix} 1 \\ 1 \\ 0 \end{pmatrix} + \begin{pmatrix} 0 \\ 1 \\ 0 \end{pmatrix} - \begin{pmatrix} 1 \\ 0 \\ 0 \end{pmatrix} = \begin{pmatrix} 0 \\ 2 \\ 0 \end{pmatrix}; \text{ one of two columns is redundant.}$$

Case2; when $B_{r,ld} = \{1 \ 0 \ 0\}$ and $B_{r,ld'} = \{1 \ 0 \ 0\}$

$$\begin{pmatrix} 1 \\ 0 \\ 0 \end{pmatrix} + \begin{pmatrix} 0 \\ 0 \\ 0 \end{pmatrix} - \begin{pmatrix} 1 \\ 0 \\ 0 \end{pmatrix} = \begin{pmatrix} 0 \\ 0 \\ 0 \end{pmatrix} \quad \begin{pmatrix} 1 \\ 0 \\ 0 \end{pmatrix} + \begin{pmatrix} 0 \\ 0 \\ 0 \end{pmatrix} - \begin{pmatrix} 1 \\ 0 \\ 0 \end{pmatrix} = \begin{pmatrix} 0 \\ 0 \\ 0 \end{pmatrix}; \text{ one of two columns is redundant.}$$

Case3; when $B_{r,ld} = \{1 \ 0 \ 0\}$ and $B_{r,ld'} = \{0 \ 1 \ 1\}$

$$\begin{pmatrix} 1 \\ 0 \\ 0 \end{pmatrix} + \begin{pmatrix} 1 \\ 1 \\ 1 \end{pmatrix} - \begin{pmatrix} 0 \\ 1 \\ 1 \end{pmatrix} = \begin{pmatrix} 2 \\ 0 \\ 0 \end{pmatrix} \quad \begin{pmatrix} 0 \\ 1 \\ 1 \end{pmatrix} + \begin{pmatrix} 1 \\ 1 \\ 1 \end{pmatrix} - \begin{pmatrix} 1 \\ 0 \\ 0 \end{pmatrix} = \begin{pmatrix} 0 \\ 2 \\ 2 \end{pmatrix}; \text{ none is redundant.}$$

Case4; when $B_{r,ld} = \{1 \ 1 \ 0\}$ and $B_{r,ld'} = \{0 \ 1 \ 1\}$

$$\begin{pmatrix} 1 \\ 1 \\ 0 \end{pmatrix} + \begin{pmatrix} 1 \\ 0 \\ 1 \end{pmatrix} - \begin{pmatrix} 0 \\ 1 \\ 1 \end{pmatrix} = \begin{pmatrix} 2 \\ 0 \\ 0 \end{pmatrix} \quad \begin{pmatrix} 0 \\ 1 \\ 1 \end{pmatrix} + \begin{pmatrix} 1 \\ 0 \\ 1 \end{pmatrix} - \begin{pmatrix} 1 \\ 1 \\ 0 \end{pmatrix} = \begin{pmatrix} 0 \\ 0 \\ 2 \end{pmatrix}; \text{ none is redundant.}$$

Finally, in order to satisfy the degree of freedom in ethane tri-reforming, the below constraints is newly added to the previous NLP model in chapter 3.6. This constraint can be valid for the equilibrium model. Eq. (4.2.c1) is meaning that at least one ξ_r in the linear dependence combination $B_{r,ld}$ are assigned zero. Through these constraints, the number of variable ξ_r can be reduced without violating any thermodynamics formulations.

$$\prod_r \xi_r = 0 \quad \text{if } B_{r,ld} = 1 \quad \text{for } ld \in LD \quad (4.2.c1)$$

$$\text{Objective; minimize } A_{ld} \quad (4.2.c2)$$

Solver for NLP model; BARON (23)

Details in Appendix C; $ST_{r,i}^{Matrix}$ and $B_{r,ld}$ for ethane tri-reforming are attached.

4.3 Results for Methanol Synthesis and Ethane Reforming

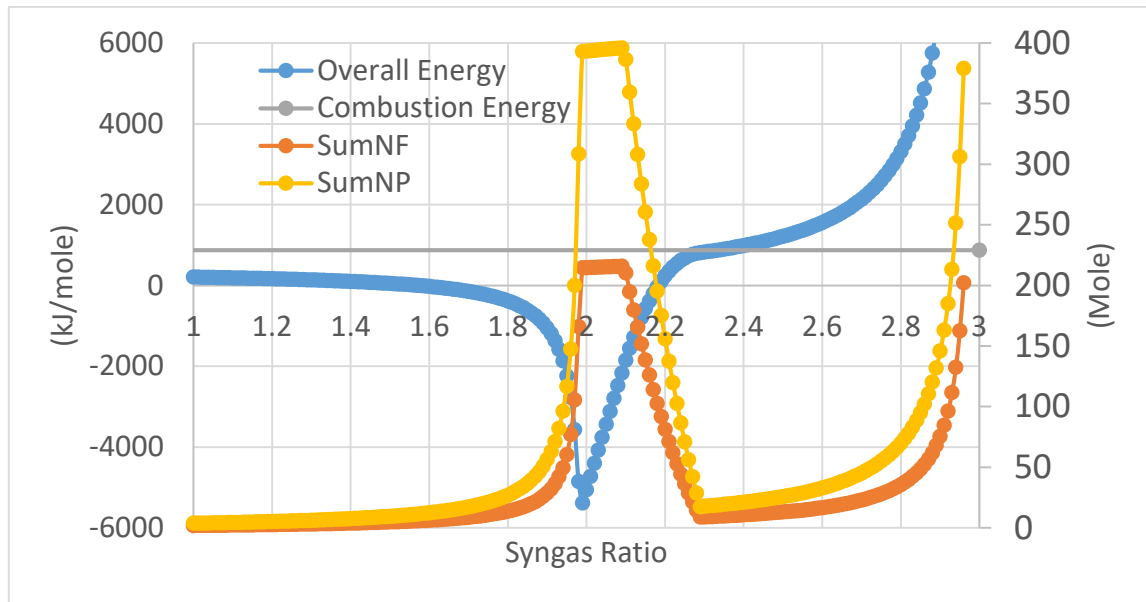
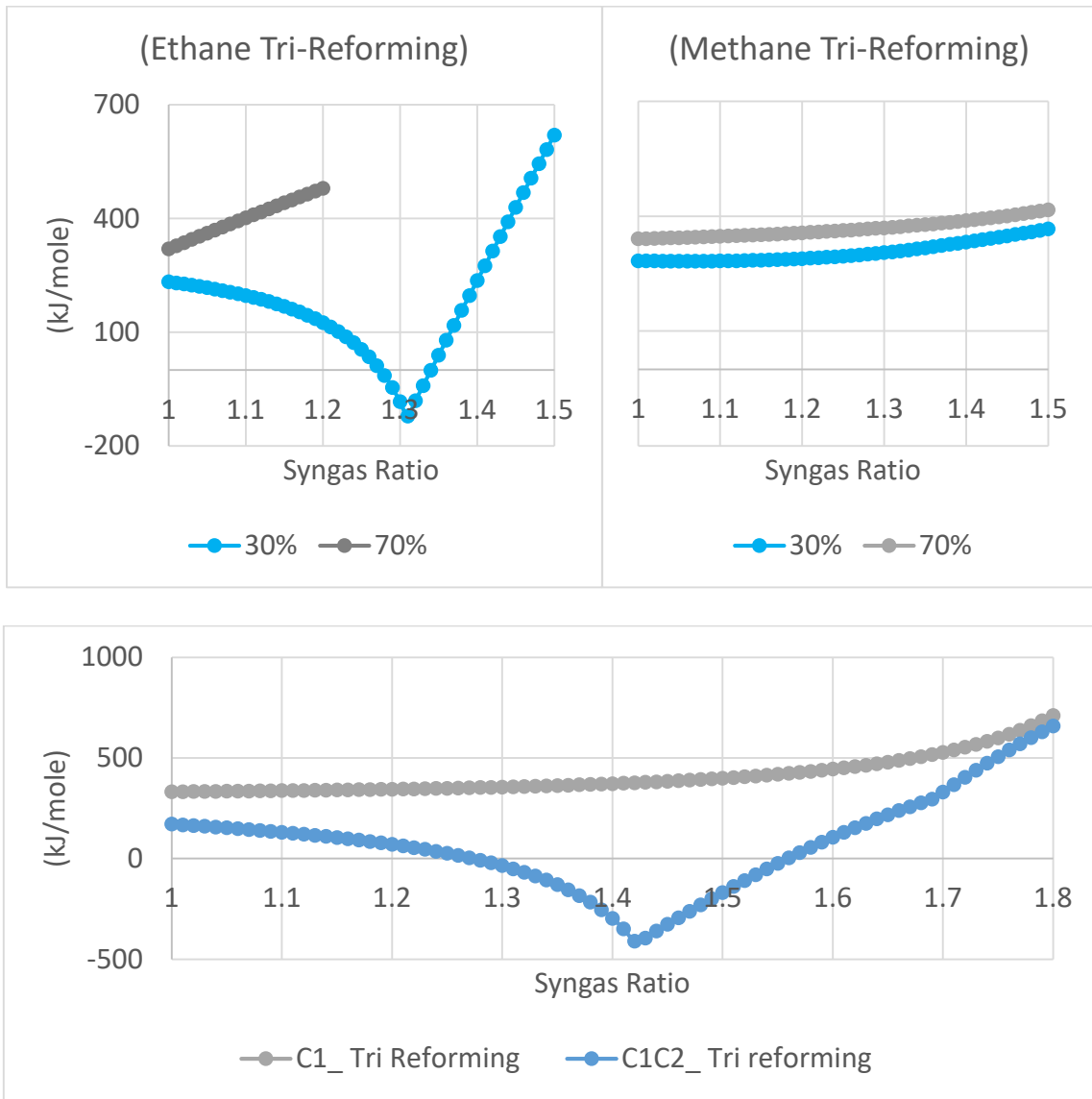


Figure 5 Results from the energetic analysis for methanol synthesis and reforming.

Figure 5 Continued



(From up to down) ¹⁾ Thermodynamically minimum energy requirement (kJ) per CO₂ utilization (moles) in the case of methanediol synthesis. CO₂ utilization is fixed as 0.9 mole (90 %). ²⁾ Thermodynamically minimum energy requirement (kJ) per CO₂ utilization (moles) in the case of ethane tri-reforming (Left) and methane tri-reforming (Right). Percentage in legend label is meaning the fixed value of CO₂ utilization. 1 percent of CO₂ utilization is meaning 0.01 mole of CO₂ utilization. ³⁾ Thermodynamically minimum energy requirement (kJ) per CO₂ utilization (moles) in the case of mixed_and_single-hydrocarbons. C1 means methane and C1C2 means combination of methane and ethane. CO₂ utilization is fixed as 0.5 mole (50 %).

In the figure of methanol synthesis, the minimum overall energy requirement, defined as summation of methanol-reforming energy and methanol-synthesis energy, is always lower than the minimum energy requirement of methane tri-reforming. At the syngas ratio of 2, the overall energy is -5.38 MJ per moles of CO₂ utilized, but the energy required for methane tri-reforming is about 13 MJ. This trade-off is caused by the fact that the larger syngas is produced, the large energy is generated from methanol reactor. For example, at the syngas ratio of 2, summation of feeds mole in the figure 4.1 is 215.14 moles, and that in the figure 3.2 is 5.63 moles.

If the objective is set as minimizing the energy requirement of methane tri-reforming just same as the figure 3.1, the overall energy combined with the reforming and the methanol reactor is 563 kJ/mole at the syngas ratio of 2, which is lower than the combustion enthalpy of natural gas. In this regard, the energy requirement in the reforming can be offset by the methanol reactor, but the trade-offs should be considered carefully.

Next, in the case of ethane tri-reforming and methane tri-reforming, energetic analysis is conducted with different CO₂ utilization constraints (30 %, 70 %). Followings are remarkable in case of ethane tri-reforming. At first, possible range of syngas ratio with high CO₂ utilization (70 %) are lower than 1.2. This is related to the stoichiometric coefficient of ethane reforming. In addition, the difference of the minimum energy requirement between high and low CO₂ utilization constraints is significantly larger than that in the methane tri-reforming. This is because exothermic reaction enthalpy of ethane combustion is large, compared to methane combustion. In other words, at same CO₂ utilization, the energy requirement of ethane is lower than that in methane tri reforming.

Therefore, at the third figure, it has been proved that the combination of reformed-hydrocarbons with methane and ethane are very effective for achieving low energy requirement unless CO₂ utilization constraint is not that high.

CHAPTER V

CONCLUSION

Combined Tri-reforming of methane have the advantages of CO₂ utilization, free-coke deposition, and syngas production. NLP model is formulated under the assumptions of ideal gas state and gas-phase reactions, and carefully using enthalpy and entropy calculation. With novelty of this mathematical modeling, this model is able to find optimal operating- conditions of temperature and feed composition.

In order to find optimal feed composition and minimum energy requirement with respect to syngas ratio, constraints are applied in this model. Gibbs free minimization for unknown feed amounts and Mole balances with extent of reactions. At the syngas ratio of 2, E_{Req}/U_{CO_2} is 979 kJ/mole where U_{CO_2} is 90 %, and meaning indirect emission of CO₂.

Through using MINLP model, overall energy requirement in the multi-step reactors of methane reforming and methanol synthesis at the syngas ratio of 2 is significantly reduced; however, the energy requirements at the methane reforming and methanol synthesis are trade-offs. This is because the larger the syngas generated at the first reactor the larger the energy generated from methanol synthesis.

The current model can be applied to large chemical model, combined with MINLP model to search linear dependence of reaction pathways, and relaxing the lackness of constraints. Ethane tri-reforming is competitive for achieving low energy requirement at the mid-range of syngas ratio. Combination of reformed-hydrocarbons are able to get high CO₂ utilization with low energy consumption.

REFERENCES

1. Ciferno J, Litynski J, Plasynski S, Murphy J, Vaux G, Munson R, et al. DOE/NETL carbon dioxide capture and storage RD&D roadmap. National Energy Technology Laboratory, accessed September. 2010;13:2011.
2. Day D, Evans RJ, Lee JW, Reicosky D. Economical CO₂, SO_x, and NO_x capture from fossil-fuel utilization with combined renewable hydrogen production and large-scale carbon sequestration. *Energy*. 2005;30(14):2558-79.
3. Change IPoC. *Climate change 2014: mitigation of climate change*: Cambridge University Press; 2015.
4. Milani D, Khalilpour R, Zahedi G, Abbas A. A model-based analysis of CO₂ utilization in methanol synthesis plant. *Journal of CO₂ Utilization*. 2015;10:12-22.
5. Biedermann P, Grube T, Höhle B. *Methanol as an energy carrier*: Forschungszentrum, Zentralbibliothek; 2006.
6. Ott J, Gronemann V, Pontzen F, Fiedler E, Grossmann G, Kersebohm DB, et al. *Methanol*. Ullmann's encyclopedia of industrial chemistry. 2012.
7. Spath PL, Dayton DC. Preliminary screening--technical and economic assessment of synthesis gas to fuels and chemicals with emphasis on the potential for biomass-derived syngas. National Renewable Energy Lab., Golden, CO.(US); 2003.
8. Balasubramanian P, editor *CO₂ capture and conversion to syngas: rigorous modeling optimization and superstructure-based process synthesis 2017*; College Station: Texas A&M University.

9. How much carbon dioxide is produced when different fuels are burned? 2017 [Available from: <https://www.eia.gov/tools/faqs/faq.php?id=73&t=11>].
10. O'Connor AM, Ross JR. The effect of O₂ addition on the carbon dioxide reforming of methane over Pt/ZrO₂ catalysts. *Catalysis Today*. 1998;46(2-3):203-10.
11. Amin NAS, Yaw TC. Thermodynamic equilibrium analysis of combined carbon dioxide reforming with partial oxidation of methane to syngas. *International Journal of Hydrogen Energy*. 2007;32(12):1789-98.
12. Lee S-H, Cho W, Ju W-S, Cho B-H, Lee Y-C, Baek Y-S. Tri-reforming of CH₄ using CO₂ for production of synthesis gas to dimethyl ether. *Catalysis Today*. 2003;87(1-4):133-7.
13. Song C, Pan W. Tri-reforming of methane: a novel concept for catalytic production of industrially useful synthesis gas with desired H₂/CO ratios. *Catalysis Today*. 2004;98(4):463-84.
14. Cho W, Song T, Mitsos A, McKinnon JT, Ko GH, Tolsma JE, et al. Optimal design and operation of a natural gas tri-reforming reactor for DME synthesis. *Catalysis Today*. 2009;139(4):261-7.
15. Joo O-S, Jung K-D, Moon I, Rozovskii AY, Lin GI, Han S-H, et al. Carbon dioxide hydrogenation to form methanol via a reverse-water-gas-shift reaction (the CAMERE process). *Industrial & engineering chemistry research*. 1999;38(5):1808-12.
16. Jeong HH, Yelleswarapu VR, Yadavali S, Issadore D, Lee D. Kilo-scale droplet generation in three-dimensional monolithic elastomer device (3D MED). *Lab Chip*. 2015;15(23):4387-92.
17. Conchouso D, Castro D, Khan SA, Foulds IG. Three-dimensional parallelization of microfluidic droplet generators for a litre per hour volume production of single emulsions. *Lab Chip*. 2014;14(16):3011-20.

18. Smith J, Van Ness H, Abbott M. Chemical engineering thermodynamics. *Sat.* 1996;18:1-3.
19. Zhu J, Zhang D, King K. Reforming of CH₄ by partial oxidation: thermodynamic and kinetic analyses. *Fuel.* 2001;80(7):899-905.
20. Bartholomew CH. Carbon Deposition in Steam Reforming and Methanation. *Catalysis Reviews.* 1982;24(1):67-112.
21. Nikoo MK, Amin N. Thermodynamic analysis of carbon dioxide reforming of methane in view of solid carbon formation. *Fuel Processing Technology.* 2011;92(3):678-91.
22. Misener R, Floudas CA. ANTIGONE: algorithms for continuous/integer global optimization of nonlinear equations. *Journal of Global Optimization.* 2014;59(2-3):503-26.
23. Sahinidis NV. BARON: A general purpose global optimization software package. *Journal of global optimization.* 1996;8(2):201-5.

APPENDIX A

LIST OF SUBSETS

$I_{Ref}(i)$ Subset for element and species used as reference state

$I_{Ref}(i)$ includes carbon (graphite, crystal), hydrogen gas, and oxygen gas

$IB(i)$ Subset for basic 6 species, which are mainly-feed and syngas

$IB(i) = \{Coke, CH_4, CO_2, CO, H_2, O_2, H_2O\}$

$I_{Feed}(i)$ User-decided subset containing feed species varied by reactor types

$I_{Feed}(i) = \{CH_4, CO_2, H_2O\}$ for Reactor CDSR

$I_{Feed}(i) = \{CH_4, CO_2, O_2\}$ for Reactor PODR

$I_{Feed}(i) = \{CH_4, CO_2, O_2, H_2O\}$ for Reactor CR

$I_{Prod}(i)$ User-decided subset containing product species varied by reactor types

$I_{Prod}(i) = \{Coke, CH_4, CO_2, CO, H_2, H_2O\}$ for Reactor CDSR

$I_{Prod}(i) = \{Coke, CH_4, CO_2, CO, H_2, O_2, H_2O\}$ for Reactor PODR and CR

Reactant species are often consumed totally and remain nothing, depending on composition and reactor types. Under that conditions, certain species are excluded from the I_{Prod} .

APPENDIX B

LIST OF PARATERMETERS AND VARIABLE BOUNDS

	Stoichiometric Coefficient					
	CH ₄	CO ₂	CO	H ₂	O ₂	H ₂ O
RS 1	-1	-1	2	2	0	0
RS 2	-1	0	1	2	-0.5	0
RS 3	-1	0	1	3	0	-1
RS 4	0	-1	1	-1	0	1
RS 5	-1	1	0	2	-1	0
RS 6	-1	1	0	0	-2	2
RS 7	-1	1	0	4	0	-2
RS 8	0	1	-1	1	0	-1

Table B.1 Stoichiometric coefficients in methane reforming

	C ₂ H ₆	C ₂ H ₄	CH ₄	Coke	O ₂	H ₂ O	CO ₂	CO	H ₂
CH ₄ _Dry	0	0	-1	0	0	0	-1	2	2
Ethane_Half_Dry	-1	0	1	0	0	0	-1	2	1
Ethane_Dry	-1	0	0	0	0	0	-2	4	3
CH ₄ _POX	0	0	-1	0	-0.5	0	0	1	2
Ethane_Half_POX	-1	0	1	0	-0.5	0	0	1	1
Ethane_POX	-1	0	0	0	-1	0	0	2	3
CH ₄ _Combustion	0	0	-1	0	-2	2	1	0	0
Ethane_Combustion	-1	0	0	0	-3.5	3	2	0	0
CH ₄ _Steam	0	0	-1	0	0	-1	0	1	3
Ethane_Half_Steam	-1	0	1	0	0	-1	0	1	2
Ethane_Steam	-1	0	0	0	0	-2	0	2	5
RWGS	0	0	0	0	0	1	-1	1	-1
CH ₄ _cracking	0	0	-1	1	0	0	0	0	2
Ethane_Cracking	-1	0	0	2	0	0	0	0	3
Boudard_Rxn	0	0	0	1	0	0	1	-2	0
Gasification_CO2	0	0	0	-1	0	0	-1	2	0
Gasification_O2	0	0	0	-1	-1	0	1	0	0
Gasification_H2O	0	0	0	-1	0	-1	0	1	1
Ethane_Dehydrogenation	-1	1	0	0	0	0	0	0	1

Table B.2 Stoichiometric coefficients in ethane reforming.

This page is guideline for Thermodynamic Table. This symbol-name is identical in GAMS coding.

C	the number of carbon-atom in species i
H	the number of hydrogen-atom in species i
O	the number of oxygen-atom in species i
CA	A_i Heat capacity coefficient for constant term
CB	B_i Heat capacity coefficient for linear-temperature term
CC	C_i Heat capacity coefficient for quadratic-temperature term
CD	D_i Heat capacity coefficient for inverse-quadratic term of temperature
Hf_T1	$\Delta H_{f,i}^o$ Lower bound of standard Enthalpy of formation for species 'i' at T_1
Gf_T1	$\Delta G_{f,i}^o$, Lower bound of standard Gibbs Free Energy of formation for species 'i' at
S_T1	Lower bound of standard entropy for species 'i' at T_1
Tmax	Upper bound of temperature till heat capacity coefficients are available
Rphi_max	Sensible Heat Difference between T_1 and T_2
Rpsi_max	Sensible Entropy Difference between T_1 and T_2
H_max	$H_i (T_2, P_2)$ Upper bound of standard Enthalpy for species 'i' at T_2
G_max	$\Delta G_{f,i}^o(T_2, P_2)$ Upper bound of standard Gibbs Free Energy for species 'i' at T_2
S_max	Upper bound of standard Entropy for species 'i' at T_2
Hf_max	Upper bound of standard enthalpy of formation for species 'i' at T_2
Gf_max	Upper bound of standard Gibbs free energy of formation for species 'i' at T_2
beta0	Linear Regression coefficients for Gibbs free energy of formation
beta1	Linear Regression coefficients for Gibbs free energy of formation

Chemicals & Code Name		C	H	O	CA	CB	CC	CD	Hf_T1	Gf_T1	S_T1
Carbon (Graphite)	C	1	0	0	N/A	N/A	N/A	N/A	0.00	0.00	5.74
Methane	CH4	1	4	0	1.702	9.081	-2.164	0	-74.52	-50.46	186
Carbon Dioxide	CO2	1	0	2	5.457	1.045	0	-0.031	-393.50	-394.40	213.6
Oxygen	O2	0	0	2	3.639	0.506	0	-0.227	0.00	0.00	205.2
Water (steam)	H2O	0	2	1	3.47	1.45	0	0.121	-241.82	-228.57	188.8
Carbon Monoxide	CO	1	0	1	3.376	0.557	0	-1.157	-110.50	-137.23	197.6
Hydrogen	H2	0	2	0	3.249	0.422	0	0.083	0.00	0.00	130.7
Ethane	IP01	2	6	0	1.131	19.225	-5.561	0	-84.70	-32.90	229.5
Propane	IP02	3	8	0	1.213	28.785	-8.824	0	-104.50	-23.40	269.9
Ethylene	IO01	2	4	0	1.424	14.394	-4.392	0	52.51	68.46	219
Propylene	IO02	3	6	0	1.637	22.706	-6.915	0	19.71	62.21	267
Methanol	IL01	1	4	1	2.211	12.216	-3.45	0	-200.66	-161.96	240
Ethanol	IL02	2	6	1	3.518	20.001	-6.002	0	-235.10	-168.49	283

Chemicals & Code Name		Tmax	Rphi_max	Rpsi_max	H_max	G_max	S_max	Hf_max	Gf_max	beta0	beta1
Carbon (Graphite)	C	N/A	N/A	N/A	23.3	-27.324	33.749	0	0	0	0
Methane	CH4	1500	78.506	94.16	3.986	-416.254	280.16	-92.196	74.981	-81.579	0.104
Carbon Dioxide	CO2	2000	63.846	83.603	-329.654	-775.458	297.203	-393.354	-401.36	-392.674	-0.006
Oxygen	O2	2000	40.4	52.917	40.4	-346.775	258.117	0	0	0.000	0.000
Water (steam)	H2O	2000	47.97	61.642	-193.848	-569.512	250.442	-250.49	-164.169	-244.549	0.054
Carbon Monoxide	CO	2500	36.152	45.716	-74.348	-439.322	243.316	-117.848	-238.611	-112.080	-0.084
Hydrogen	H2	3000	36.441	48.231	36.441	-231.955	178.931	0	0	0.000	0.000
Ethane	IP01	1500	132.408	157.333	47.708	-532.541	386.833	-108.215	217.972	-95.135	0.209
Propane	IP02	1500	188.832	224.646	84.332	-657.487	494.546	-131.333	352.305	-116.603	0.313
Ethylene	IO01	1500	102.784	123.499	155.294	-358.454	342.499	35.811	160.104	45.725	0.076
Propylene	IO02	1500	156.172	186.749	175.882	-504.741	453.749	-3.342	273.095	9.888	0.175
Methanol	IL01	1500	99.823	120.769	-100.837	-641.992	360.769	-217.22	22.63	-207.752	0.154
Ethanol	IL02	1500	159.139	193.188	-75.961	-790.244	476.188	-252.085	133.657	-243.445	0.251

APPENDIX C

SUPPLEMENTARY DATA

	Enthalpy of Reaction (kJ/mol) with respect to T ₂					comment
	298.15 K	600 K	900 K	1200 K	1500 K	
RS 1	247.359	219.148	185.441	147.065	104.994	Endothermic
RS 2	-35.625	-10.600	16.265	44.438	73.781	Swing
RS 3	206.203	240.000	275.835	313.288	352.234	Endothermic
RS 4	41.156	59.152	79.504	101.596	125.286	Endothermic
RS 5	-318.609	-286.228	-252.739	-217.838	-181.505	Exothermic
RS 6	-802.265	-766.395	-727.997	-686.696	-642.463	Exothermic
RS 7	165.047	214.973	266.399	319.862	375.401	Endothermic
RS 8	-41.156	-17.547	6.973	32.594	59.322	Swing

Table C.1 Enthalpy of the reaction pathways in regard with product temperature.

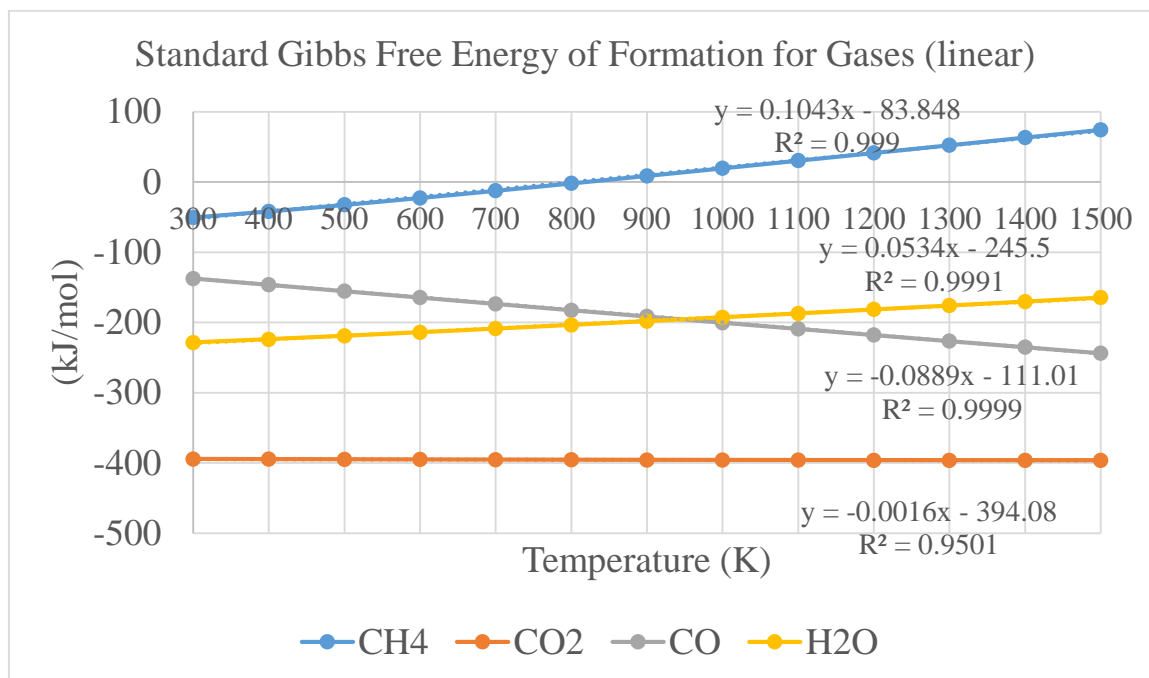


Table C.2 Linear Regression for standard Gibbs free energy of formation.